

Review

Solid Polymer Electrolytes for Zinc-Ion Batteries

Ivan Miguel De Cachinho Cordeiro ¹, Ao Li ¹, Bo Lin ¹, Daphne Xiuyun Ma ², Lulu Xu ², Alice Lee-Sie Eh ^{3,*} and Wei Wang ^{1,*}

¹ School of Mechanical and Manufacturing Engineering, University of New South Wales, Sydney, NSW 2052, Australia; i.decachinhocordeiro@unsw.edu.au (I.M.D.C.C.)

² School of Materials Science and Engineering, Nanyang Technological University, 50 Nanyang Avenue, Singapore 639798, Singapore

³ Metrohm Singapore, 31 Toh Guan Road East, #06-08 LW Techno Centre, Singapore 608608, Singapore

* Correspondence: alice.eh@metrohm.com.sg (A.L.-S.E.); wei.wang15@unsw.edu.au (W.W.)

Abstract: To date, zinc-ion batteries (ZIBs) have been attracting extensive attention due to their outstanding properties and the potential to be the solution for next-generation energy storage systems. However, the uncontrollable growth of zinc dendrites and water-splitting issues seriously restrict their further scalable application. Over the past few years, solid polymer electrolytes (SPEs) have been regarded as a promising alternative to address these challenges and facilitate the practical advancement of zinc batteries. In this review, we revisit the research progress of SPEs applied in zinc batteries in the past few years and focus on introducing cutting-edge polymer science and technologies that can be utilised to prepare advanced SPEs for high-performance zinc batteries. The operating mechanism of SPEs and the functions of polymers are summarised. To highlight the polymer's functions, SPEs are categorised into three types, homogenous polymer SPEs, hybrids polymer SPEs, and nanocomposites SPEs, which are expected to reveal the roles and principles of various polymers in zinc batteries. This review presents the current research progress and fundamental mechanisms of polymer-based SPEs in zinc batteries, outlines the challenging issues encountered, and proposes potential solutions for future endeavours.

Keywords: solid polymer electrolytes; zinc batteries; nanocomposites; zinc dendrites; ion conductivity



Citation: De Cachinho Cordeiro, I.M.;

Li, A.; Lin, B.; Ma, D.X.; Xu, L.; Eh, A.L.-S.; Wang, W. Solid Polymer Electrolytes for Zinc-Ion Batteries. *Batteries* **2023**, *9*, 343. <https://doi.org/10.3390/batteries9070343>

Academic Editor: Catia Arbizzani

Received: 31 May 2023

Revised: 17 June 2023

Accepted: 19 June 2023

Published: 27 June 2023



Copyright: © 2023 by the authors. Licensee MDPI, Basel, Switzerland. This article is an open access article distributed under the terms and conditions of the Creative Commons Attribution (CC BY) license (<https://creativecommons.org/licenses/by/4.0/>).

1. Introduction

To date, the increased consumption of fossil fuels has led to emerging environmental issues such as climate change and air and water pollution, which have garnered significant and wide attention. Over the past several decades, there has been increasing emphasis on the development of renewable energy sources and their corresponding energy storage systems. Several energy storage systems, such as lithium-ion batteries, sodium-ion batteries, lithium-air batteries, fuel batteries, and alkaline metal batteries, have been developed with outstanding performance. Among these, the research and development of rechargeable lithium-ion batteries have been particularly feasible and practical. As a result of their exceptional energy density, high voltage, and excellent cycling performance, lithium batteries have successfully been utilised in various areas, such as electric vehicles, energy storage stations, and portable electronics. Nevertheless, lithium-ion batteries are still facing some crucial challenges, for example, their high cost and fire safety issues that seriously restrict further applications. Recently, aqueous zinc-ion batteries (ZIBs) have attracted extensive attention owing to the high theoretical volume capacity of the Zn metal anode (5854 mAh cm^{-3}) [1,2], the low redox potential of Zn/Zn²⁺ ($-0.76 \text{ V vs. standard hydrogen electrode (SHE)}$) [3,4], the nontoxicity, and rich zinc resources. However, similar to lithium batteries, when using zinc metal as the anode material, ZIBs also have safety issues induced by the uncontrollable growth of zinc dendrites [5–9]. The dendrites are usually formed on the surface of anodes where the zinc ions are reduced to zinc metal,

which are like whiskers and can pierce through the separator and lead to battery short circuits and even an explosion [5–7]. In addition, the formation of zinc dendrites is usually accompanied by side chemical reactions among the electrolyte, zinc metal, and zinc salts and causes the continuous consumption of electrolyte zinc salts, which will lead to reduced capacity, low efficiency, and short lifespan. Another crucial issue is induced by the water splitting process, as the ZIBs use water as the solvent, which may lead to corrosion, hydrogen evolution reactions (HERs), and oxygen evolution reactions (OERs) [10–12]. These side reactions may lead to the continuous consumption of water and poor battery efficiency. Additionally, cathode materials of ZIBs, including MnO_2 [13,14], Prussian blue analogues [15,16], and vanadium-based oxides [17–19], could partially dissolve in aqueous electrolytes and lead to deteriorated performance. Therefore, for ZIBs to exhibit an excellent prolonged cycling lifespan and stability, many efforts have been devoted to electrolyte improvement strategies.

Solid polymer electrolytes (SPEs) have attracted significant attention in recent years as a promising alternative to liquid electrolytes in rechargeable zinc batteries [20–26]. Normally, as per the composition, SPEs are one type of polymer electrolyte (PE) that could be used to realise advanced ZIBs. There are two more PE categories that can also be applied in safe ZIBs: gel polymer electrolytes (GPEs) and hybrid polymer electrolytes (HPEs) [21,27–29]. Summarily, all three types of PEs consist of long polymer chains and zinc salts/media. In terms of SPEs, the zinc salts may be dissolved in polymer chains [23,25,30,31]. For GPEs, they are prepared by dissolving the zinc salts in solvent and obtaining the gels [32–35]. As for HPEs, they are mainly realised by crosslinking or copolymerisation methods to connect two or more types of polymer chains in which zinc salts are dispersed [29,36].

In this review, we focus on the development of solid-state polymer electrolytes for zinc-ion batteries. The remarkable advantages of SPEs, including high ionic conductivity, mechanical flexibility, and improved safety, make them ideal for use in advanced energy storage systems. There have already been some reviews introducing the development of electrolytes of zinc batteries [21,22,37,38]. However, these reviews mainly introduced the electrolytes from the aspects of cathodes/electrolytes, structure design, types of zinc batteries, and polymer types. It should be noted that in this review, we focus on the SPEs with various polymer strategies that can achieve high-performance and safe ZIBs. Additionally, when it comes to summarising the SPEs for ZIBs, we mainly include the solid-state polymer electrolytes applied in ZIBs. A few SPEs that are close to the gel-like state but have unique structures and outstanding properties are also categorised and introduced here. In detail, we discuss the properties and characteristics of SPEs, including their types, preparation methods, and ion transport mechanisms. Additionally, we review recent advances in the development of solid polymer electrolytes for zinc-ion batteries, highlighting their synthesis, performance, and limitations. Lastly, we conclude with a summary of the current status and future directions of SPEs for ZIBs.

2. Classification of SPEs

Owing to the significant research interests of ZIBs in recent decades, extensive reviews regarding ZIB chemistry have been conducted by Wu et al. [21], Zhang et al. [39], Mo et al. [22], and Wang et al. [37]. These reviews comprehensively reviewed the materials of the anode, cathode, and electrolyte, as well as the physiochemical and thermomechanical properties of different material combinations. However, the engineering of an electrolyte can be complicated as it affects the mass transport, energy storage mechanisms, and reactions of ZIBs, and the versatility of potential electrolyte materials has further increased the difficulty of reviewing ZIB electrolytes systematically. Wu et al. [21] performed an excellent review of an extensive range of polymer-based electrolytes and categorised them into solid, hydrogel, and hybrid state electrolytes. Zhang et al. [39] classified electrolytes into aqueous, aqueous gel, organic, ionic liquids, and deep eutectic solvents. In this mini-review, a wide spectrum of SPEs studies is reviewed and categorised into three groups, namely the homogenous polymer SPEs, hybrid-polymer-based SPEs, and nanocomposite polymer

electrolytes. This study aims to revisit the current state of solid-state electrolyte engineering for ZIBs, specifically on the cutting-edge technologies of SPEs utilising polymer science and technologies to realise advanced ZIBs. Unlike existing reviews, in this review, we anticipate highlighting the functions of polymers, polymer hybrids, and polymer composites inside SPEs and how these polymer systems can enhance the performance of ZIBs. This is also the reason for categorising the SPEs into three types. The discussion of homogenous polymer SPEs will help to study the research mechanism of one kind of polymer on the performance of ZIBs. In terms of hybrid-polymer-based SPEs, the illustrations will reveal the interaction between different polymer components that can promote the ion mobility and facilitate the battery properties. Lastly, polymers can also play key functions in improving the safety and performance of ZIBs along with inorganic materials. This section introduces how the inorganic/polymer nanocomposites can significantly impact the zinc ion transport and maintain a stable operating process for a long lifespan.

3. Homogenous Polymer Matrix SPEs

In the early SPE studies, organic polymer matrices such as polyethylene oxide (PEO) [40], polyvinylidene fluoride (PVDF) [41], polyacrylamide (PAM) [42], and polyvinyl alcohol (PVA) [43] were widely adopted with a low-molecular-weight plasticiser to enhance the ionic conductivity of the electrolytes. Nonetheless, these polymers were commonly reported with low ionic conductivity and poor interface compatibility. For instance, as one of the most common electrolyte materials for LIBs and ZIBs, the flexible chains of PEO have allowed Zn^{2+} ions to be transferred by segmental motion [44]. However, efficient Zn^{2+} conduction and zinc electrochemistry have been challenging to achieve owing to the high degree of crystallisation of PEO and its interfacial incompatibility with Zn metal. This leads to the poor ionic conductivity of PEO, reported as approximately 1.09×10^{-6} to $2.87 \times 10^{-5} \text{ S cm}^{-1}$ at room temperature. To enhance the ion transfer, Zhao et al. [45] utilised poly(ethylene glycol) methyl ether acrylate (PEGMEA) to synthesise in situ-polymerised PEO-based SPEs. This approach formulated a cross-linking structure within the amorphous regime and improved the ionic conductivity to $2.87 \times 10^{-5} \text{ S cm}^{-1}$, as revealed in Figure 1a. Except for overcoming the poor interfacial ion transport, the in situ strategy also improves the reversibility of Zn electrochemistry in symmetrical cells. Except for PEO, Poly(vinylidene fluoride) (PVdF) is one of the common electrolytes in ZIB development owing to its porous semicrystalline structures, where the strong electron-withdrawing effect can be observed at the CF_2 functional groups. This accelerates the isolation of the metal salts, increasing the number of charges that contributes to the ionic conductivity [46]. Song et al. [31] utilised solution casting methods to synthesise PVdF-HFP (poly(vinylidene fluoride-hexafluoropropylene))-based SPEs, where an ionic conductivity of $2.44 \times 10^{-5} \text{ S cm}^{-1}$ was achieved at room temperature, with a mass ratio of 0.4 between $\text{Zn}(\text{Tf})_2$ and PVdF-HFP. Furthermore, the intrinsic structure of PVdF-HFP also allows the flow of charge through complexation and decomplexation within the polymer segments, as depicted in Figure 1b. Nevertheless, PVDF possesses similar drawbacks to PEO, where low ionic conductivity, high interfacial resistance, rapid degradation, and poor mechanical strength can be observed in early ZIB studies [39].

To overcome the addressed drawbacks of conventional SPEs, especially low ionic conductivity and high interfacial resistance, Ma et al. [26] reported an amorphous SPE via in situ ring-opening polymerisation of a precursor of 1,3-dioxolane (DOL) within an electrochemical cell, as shown in Figure 2a. This synthesis method led to the incorporation of a substantial concentration of zinc salts into the SPE matrix. The in situ-formed SPEs demonstrated a high ion conductivity of $1.96 \times 10^{-2} \text{ S cm}^{-1}$ at room temperature and non-dry properties. Owing to the well-connected pathways and lesser interfacial defects, only 10% interfacial impedance was retained compared to a conventional battery, leading to a higher columbic efficiency. Moreover, the developed battery successfully achieved charging/discharging cycles of 1800 h without dendrite growth. To further strengthen the ionic conductivity and mechanical properties, Liu et al. [23] synthesised dry polymer

“PHP” by introducing a 2,6-bis((propylimino)methyl)-4-chlorophenol (Hbimcp) ligand into the poly(propylene oxide) (PPO) polymer chain, where the SPE film is obtained after being slowly volatilised in a polytetrafluoroethylene mould at room temperature. The PHP SPE was reported with a moderate ion conductivity of 10^{-5} S cm^{-1} and significant flexibility at 1000% elongation strain and a fast self-healing capability. Also, the ZIB exhibited a remarkable cycling stability (125% capacity retention after 300 cycles) and a high coulombic efficiency (94% after 300 cycles). These favourable properties can be attributed to the unique coordination system of PHP, where the strong coordination withstands stress during stretching while the fast ligand exchange between zinc ions and the PHP polymer chains endows ion conductivity. Moreover, the imine bonds in the polymer also enable acidic degradation of the electrolyte that improves its recyclability.

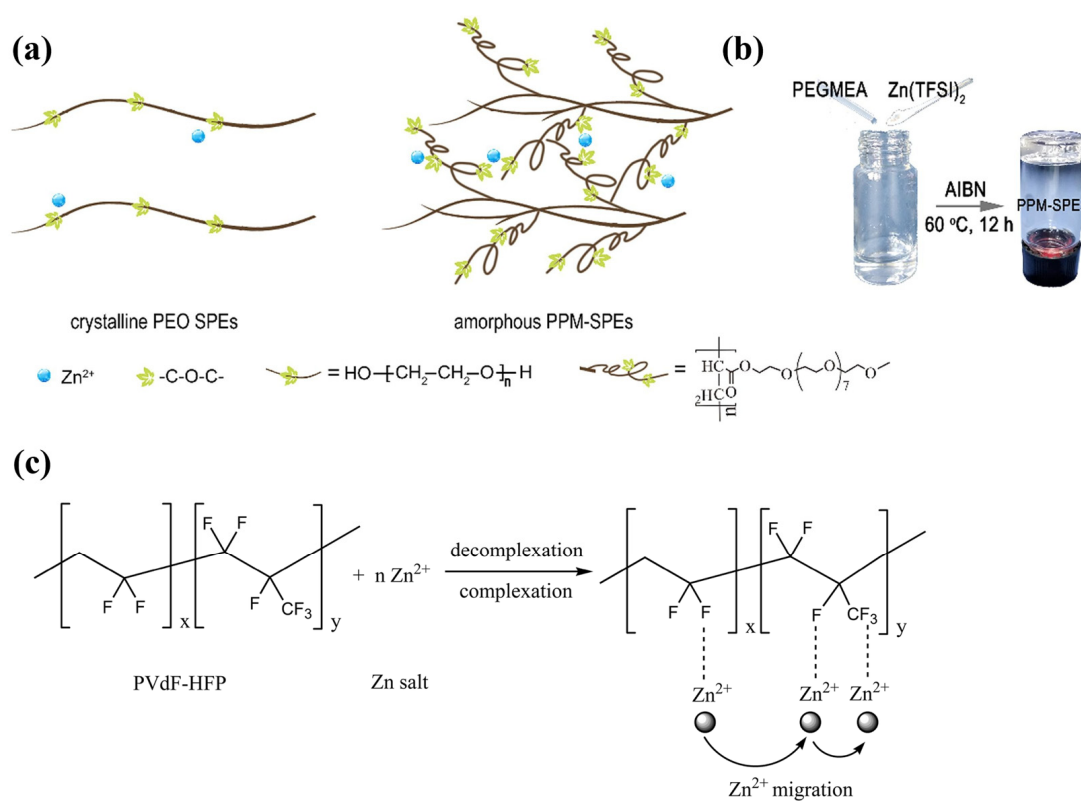


Figure 1. (a) The schematics of PEO-based SPEs and amorphous PPM-SPEs. Reproduced with permission from [45]. (b) The synthesis of PPM-SPEs. (c) The schematic of Zn²⁺ transport mechanism. Reproduced with permission from [31].

Except for electromechanical and cost efficiency, environmentally friendly and recyclable energy storage devices are also vital to establish a positive transition towards sustainable energy storage. Brige et al. [2] fabricated bio-based SPEs utilising hydroxyethylcellulose (HEC), an amorphous homogenous biopolymer. HEC contains side chains composed of ethylene oxide groups that are grafted onto the cellulose backbone. As a result, despite HEC possessing favourable film-forming characteristics, comparable to PEO, the low capability of salt-dissociation of HEC caused a poor ion conductivity of 10^{-6} S cm^{-1} . In order to enhance the electromechanical performance of bio-based SPEs, Huang et al. [47,48] developed bio-based SPEs by introducing kappa-carrageenan and guar gum for flexible Zn-MnO₂ batteries, which are eco-friendly, low-cost, and highly conductive. Figure 3a,b presents the molecular formula of kappa-carrageenan and the photograph of kappa-carrageenan electrolyte. By mixing the biomass with a ZnSO₄ and MnSO₄ mixture solution, the kappa-carrageenan electrolytes exhibited an excellent ion conductivity of 3.32×10^{-2} S cm^{-1} , fast charging and discharging capability (120.0 mAh g^{-1} at 6.0 A g^{-1}), impressive cycling stability (80% remaining after 450 cycles), and moder-

ate bending durability (95% after 300 cycles). Furthermore, the mechanical stiffness of the SPE was also reinforced by employing rice paper as a scaffold. While the guar-gum-electrolyte-based flexible quasi-solid-state (QSS) ZIB (Figure 3c) delivered an enhanced flexibility and conductivity compared to kappa-carrageenan, the eco-friendly electrolyte had an astonishing ion conductivity of $1.07 \times 10^{-2} \text{ S cm}^{-1}$ at ambient, which is greater than conventional quasi-solid-state polymer electrolytes. The QSS ZIB also delivered a fast charging and discharging capability (131.6 mAh g^{-1} at 6.0 A g^{-1}) and effective zinc dendrites suppression during cycling, as revealed in Figure 3d. Especially, the ZIB achieved an outstanding cycling stability, retaining 100% of its capacity after 1900 cycles and 85% after 2000 cycles, for a Zn stripping/plating testing time more than 300 hours as shown in Figure 3e. The ZIB also exhibited remarkable durability when subjected to bending, maintaining 81.3% of its capacity after undergoing 180° bending for 1000 cycles. The biopolymer electrolytes synthesised by Huang et al. exhibited significant potential for a bio-based electrolyte of high-performance ZIBs and achieved an outstanding ion conductivity and cycling performance for SPE-based ZIBs.

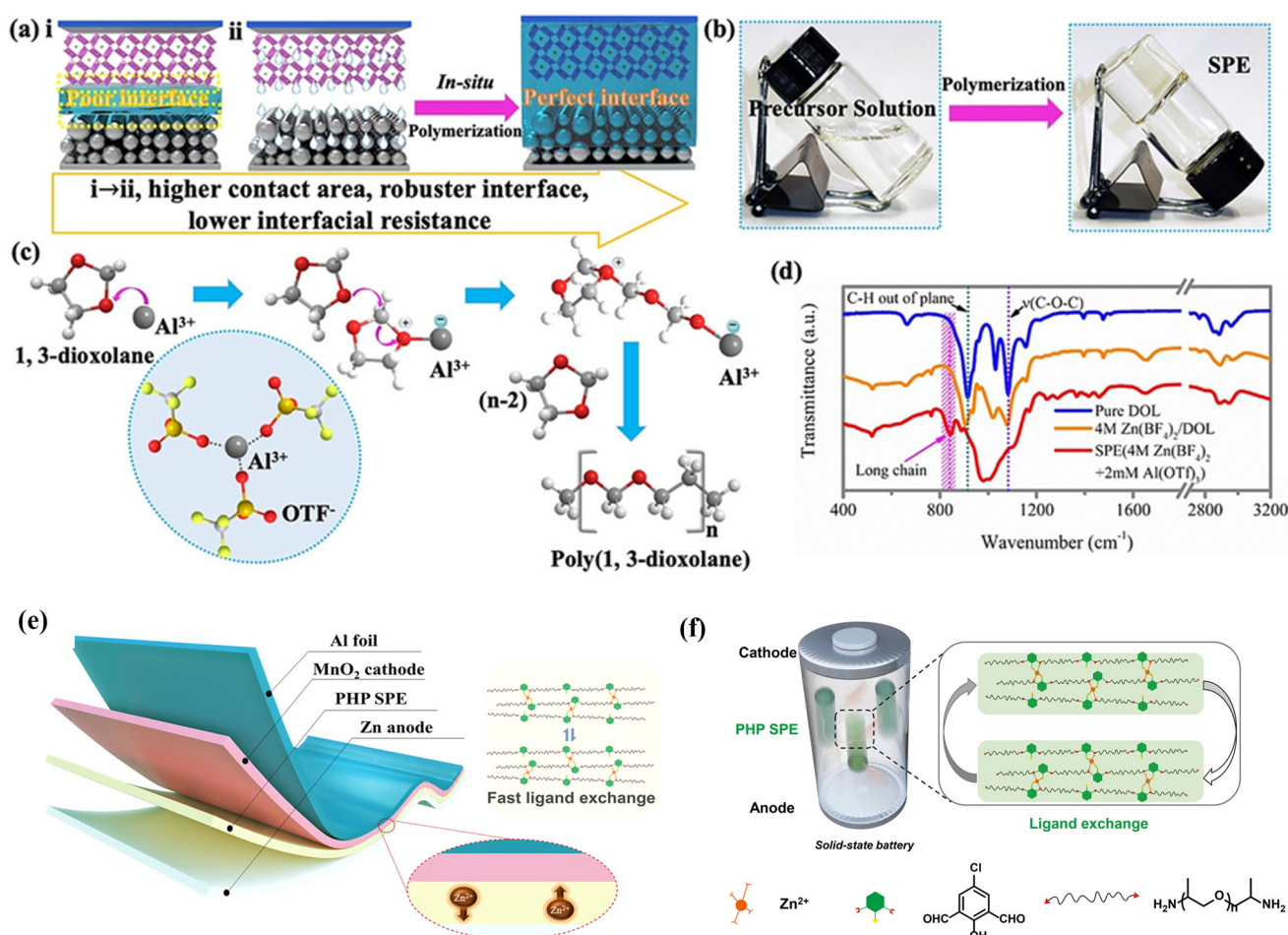


Figure 2. (a) Schematic illustration of in situ-formed SPEs for Zn batteries. (b) Photos of polymerisation process. (c) Illustration of the polymerisation mechanism of DOL. (d) The FT-IR spectrum of pure DOL, $\text{Zn}(\text{BF}_4)_2/\text{DOL}$ solution, and SPE. Reproduced with permission from [26]. (e) Schematic of the fast ligand exchange within the PHP-based ZIB. (f) The zinc ion conduction mechanism within the PHP-SPE-based all-solid-state battery. Reproduced with permission from [23].

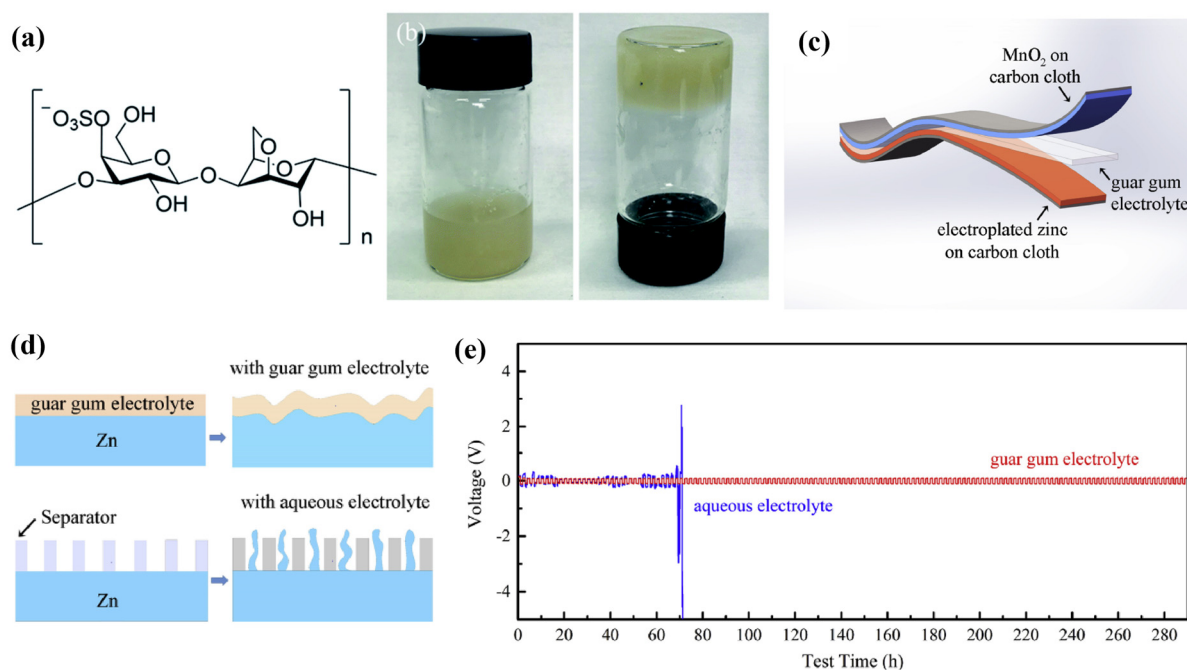


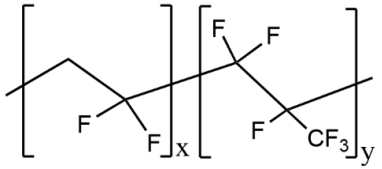
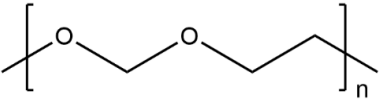
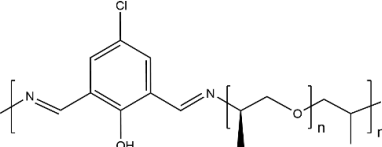
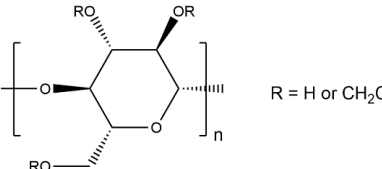
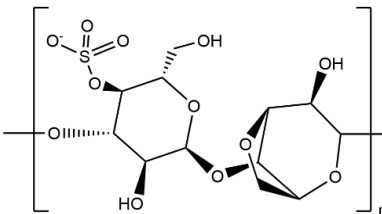
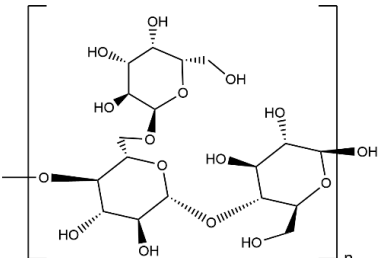
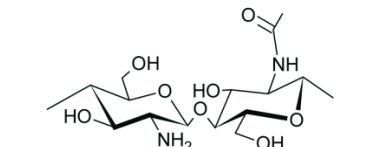
Figure 3. (a) The molecular formula of kappa-carrageenan. (b) Photograph of kappa-carrageenan electrolyte after adding 2 M ZnSO₄ and 0.1 M MnSO₄ aqueous solutions. Reproduced with permission from [47]. (c) Schematic illustration of the structure of the solid-state Zn–MnO₂ battery. (d) Schematic diagram of the morphology change of the zinc foil in guar gum electrolyte and aqueous electrolyte after cycling. (e) Zn stripping/plating from Zn/Zn symmetrical cells at 0.24 mA cm^{−2} in guar gum electrolyte and aqueous electrolyte. Reproduced with permission from [48].

Table 1 summarises the reviewed literature and studies in this section, including their molecular structures, ionic conductivity, features, and the published year. In early SPE research, conventional homogenous SPEs were reported with low ionic conductivity due to the limited segmental mobility, insufficient ion transportation pathway, and morphological limitations. To address these drawbacks, a range of advanced material engineering is reviewed in this section. One of the major approaches is in situ modifications of the polymer matrix via polymerisation [23,26,45], which enhances the amorphicity of the polymer matrix, thus providing an extra ion transportation channel and fast ligand exchanges. The other approach would be adopting bio-based polymers, such as kappa-carrageenan [47] and chitosan [49]. These biopolymers generally offer great ionic conductivity during their application in quasi-solid-state ZIBs, owing to their high segmental mobility and flexible polymer chains, also with stretchability and dendrite suppression performance [48]. Furthermore, characteristics such as non-flammability, biodegradability, and eco-friendliness can also be found with these biopolymers.

Table 1. The molecular structure, ionic conductivity, and features of homogenous polymer matrix electrolyte.

Name	Molecule Structure	Ionic Conductivity (S cm ^{−1})	Features	Year, Ref
PEO-PPM		2.87×10^{-5}	<ul style="list-style-type: none"> • Low interfacial resistance • All-solid-state 	2021, [45]

Table 1. Cont.

Name	Molecule Structure	Ionic Conductivity (S cm ⁻¹)	Features	Year, Ref
PVdF-HFP		2.44×10^{-5}	<ul style="list-style-type: none"> • Thermal stability • Electrochemical stability • Quasi-solid-state 	2020, [31]
Poly(1,3-dioxolane)		1.96×10^{-2}	<ul style="list-style-type: none"> • Cycling cyclability • Stretchable • All-solid-state 	2020, [26]
PHP		6×10^{-6}	<ul style="list-style-type: none"> • Cycling stability • High coulombic efficiency • All-solid-state 	2021, [23]
HEC	 R = H or CH ₂ CH ₂ OH	1×10^{-6}	<ul style="list-style-type: none"> • Solubility • All-solid-state 	2022, [2]
Kappa-Carrageenan		3.32×10^{-2}	<ul style="list-style-type: none"> • Eco-friendly • Fast charging • Quasi-solid-state 	2019, [47]
Guar Gum		1.07×10^{-2}	<ul style="list-style-type: none"> • Eco-friendly • Fast charging • Cycling cyclability • Quasi-solid-state 	2019, [48]
Chitosan		7.2×10^{-2}	<ul style="list-style-type: none"> • Hydrogel • Coulombic efficiency of 99.7% after 1000 cycles 	2022, [49]

4. Hybrid Polymer Matrix SPEs

The engineering of high-performance SPEs is complex and challenging as the electrolyte has to be conductive with a high charging/discharging capability and capacity retention, as well as mechanically stretchable or stiff to be flexible according to applications. However, it is rare to discover homogeneous materials with all the aforementioned properties. Hence, SPEs composed of hybrid polymer matrices have gained significant research interest, where the polymers are often synthesised through crosslinking, self-assembly, or copolymerisation. With various combinations of polymer matrices, this could grant SPEs with favourable properties, such as efficient ion transportation in amorphous structures, crosslinking reinforcement in mechanical robustness, and a flame-retardant mechanism.

Some of the pioneering works can be found in the SPE study conducted by Ye and Xu [50], where PVDF-HFP was combined with poly(ethylene glycol) dimethyl ethers (PEGDMEs) via the solution casting method. The polymer/polymer matrix revealed that PEGDME possesses significant salt solvation, while the blending of PVDF-HFP provides mechanical support, resulting in an ionic conductivity at $1.7 \times 10^{-2} \text{ S cm}^{-1}$ in ZIB composed of 0.5 M $\text{Zn}(\text{TFSI})_2/\text{PEGDME}/\text{PVDF-HFP}$. However, drawbacks such as cyclability and large weight loss leading to an ion conductivity decrement had yet to be investigated in the early work. Rathika et al. [51] employed a similar blending approach to synthesise a 90 wt% PEO/10 wt% PVdF blended polymer electrolyte with 15 wt% zinc triflate salt ($\text{Zn}(\text{CF}_3\text{SO}_3)_2$), as illustrated in Figure 4a. The blending of the polymer/polymer interface led to an amorphous phase, reducing the crystallinity of the host polymer blend matrix. This amorphous structure, as depicted in Figure 4b, facilitates the establishment of ion-polymer interactions between the polymer matrix and zinc triflate salt. The presence of this unique amorphous structure reduces the cohesive forces acting upon the polymer blend chains, allowing for increased segmental mobility. This enhanced mobility of segments within the polymer blend electrolyte system promotes improved charge mobility, thereby facilitating the movement of charges through the electrolyte.

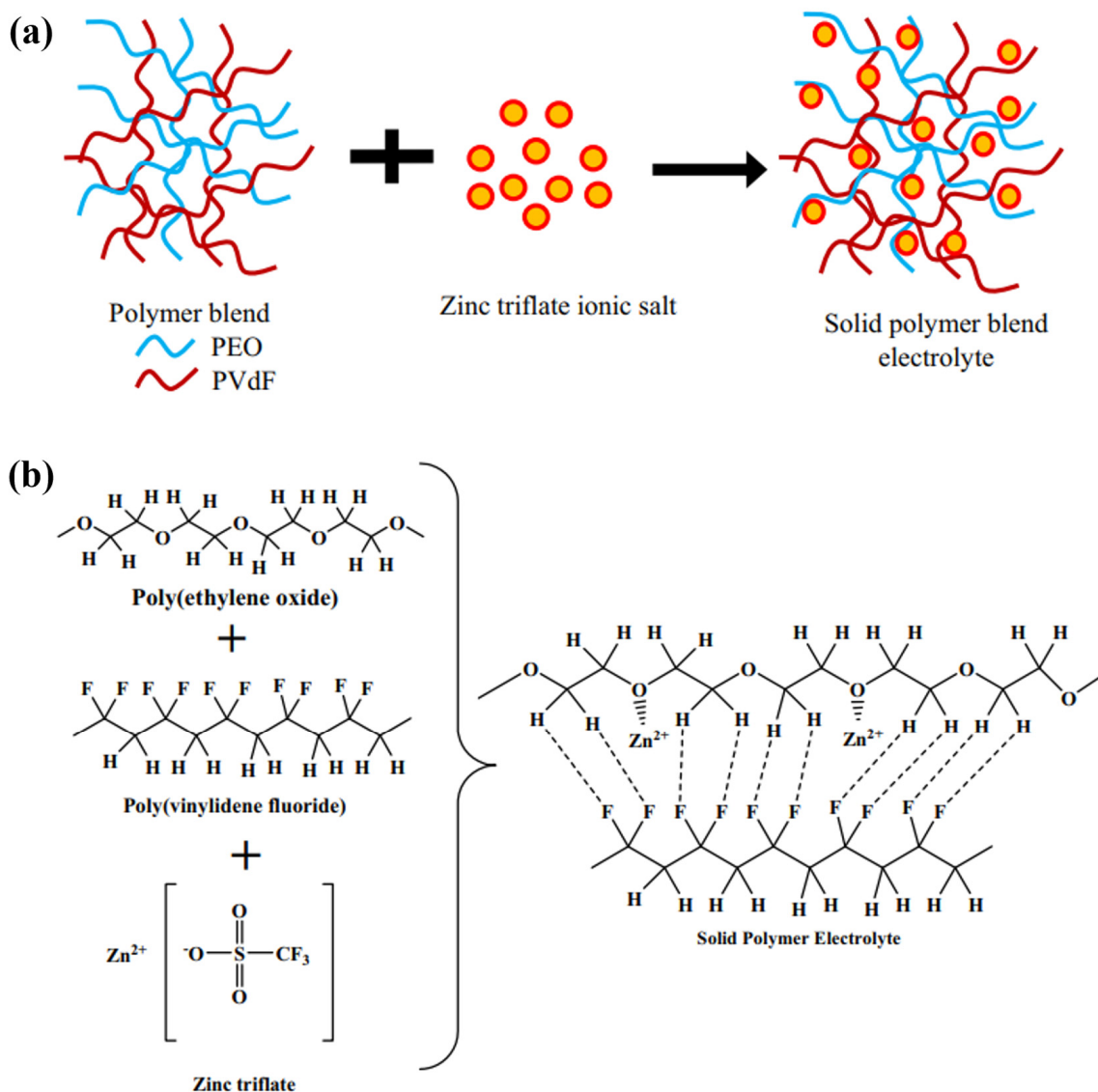


Figure 4. (a) The illustration of the formation mechanism of PEO/PVDF-blended SPEs. (b) Schematic of crosslinking and ion-polymer interactions. Reproduced with permission from [51].

Except for polymer blending, Lu et al. [52] proposed the synthesis approach of manipulating the heteroleptic coordination that integrates polyacrylamide (PAAM) ligands with acetamide coligands for zinc ion centres. As illustrated in Figure 5, the in situ catalytic polymerisation initiated by Lewis-acidic Deep eutectic solvents (DESs) significantly enhanced the mobility of Zn^{2+} and the polymer by enabling the formation of eutectic ion channels with both labile Zn^{2+} –polymer bonding. The heteroleptic coordination polymer electrolytes (HCPEs) exhibited an ionic conductivity of $4.7 \times 10^{-3} \text{ S cm}^{-1}$ and a Zn^{2+} transference number of 0.44 at room temperature, attributed to the ligand exchange process to accelerate long-range Zn^{2+} transport. The increment in available distinct ligands in the limited metal coordination sphere not only established a well-lubricated ion channel to reduce the ionic migration barrier, but it also produced a flexible coordination sphere to enable fast ligand exchange. The solid-state ZIB also performed reversibility of the Zn plating/stripping process (1200 h), with a cyclability of 350 cycles with Mo_6S_8 cathodes and a coulombic efficiency of $\sim 99\%$. Furthermore, the HCPEs exhibited remarkable flexibility and high stretchability, functioning as elastomers rather than mechanically rigid structures. Notably, these HCPEs demonstrate an impressive maximum stretchability exceeding 800% when subjected to a stretching speed of 20 mm/min. This exceptional stretchability can be attributed to the enhanced dynamics of ligand exchange within the HCPEs.

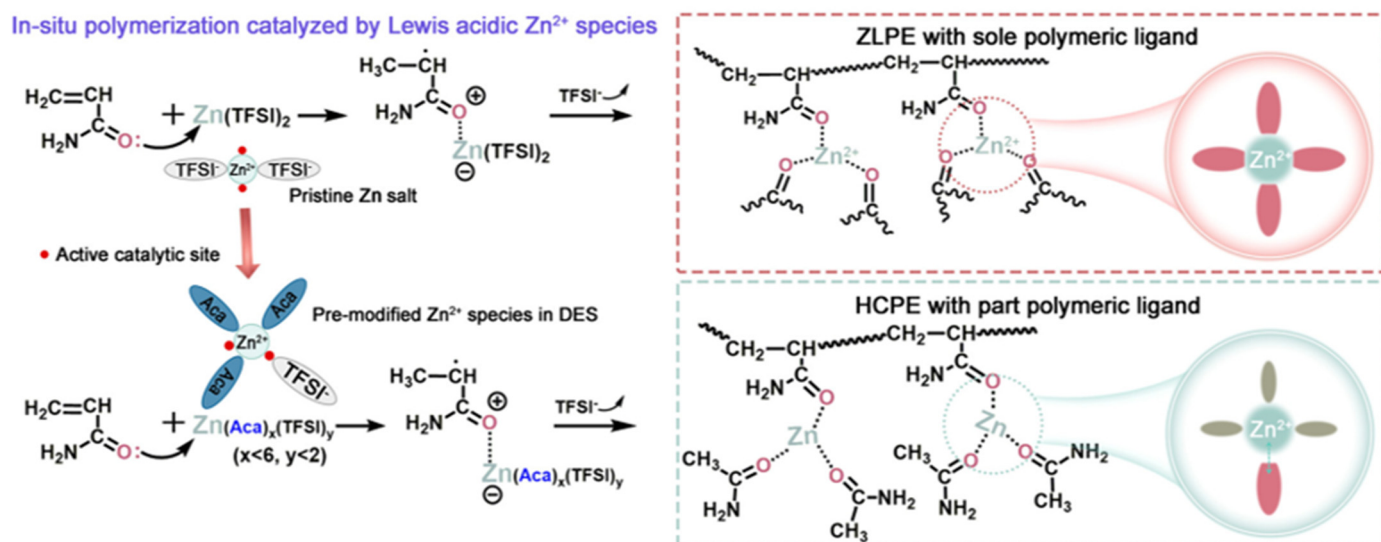


Figure 5. Schematic diagram of the concept of ZLPE and HCPEs. Reproduced with permission from [52].

Other than hybrid polymer composition, the inclusion of a bio-based polymer into the hybrid polymer matrix was often adopted in SPE research, as the biopolymer offers mechanical support, biocompatibility, and environmental friendliness. Li et al. [53] introduced a novel approach for developing a hierarchical polymer electrolyte (HPE) using gelatin and polyacrylamide (PAM) as the base materials, coupled with an α - MnO_2 nanorod and carbon nanotube (CNT) cathode. Figure 6 illustrates the synthesis route of the HPE, which was synthesised by grafting PAM onto gelatin chains that are filled in the network of a polyacrylonitrile (PAN) electrospun fibre membrane. The grafting process is achieved through a free radical polymerisation method, enabling the fabrication of the HPE. The porous hierarchical structure and significant water retention capability of the polymeric network offered an impressive ionic conductivity of $1.76 \times 10^{-2} \text{ S cm}^{-1}$, while the superior interfacial contact between the electrodes and HPE endowed enhanced ion diffusion and higher reaction kinetics for long-term cycling (capacity retention of 97% after 1000 cycles at 2772 mA g^{-1}). Moreover, the grafting of PAM onto a gelatin hydrogel (gelatin-g-PAM) offered favourable mechanical strength and excellent capacity retention (averaging above 90%) after undergoing several destructive conditions, including being cut, bent, hammered,

punctured, burnt, sewed using a commercial sewing machine, and even rinsed without any packaging.

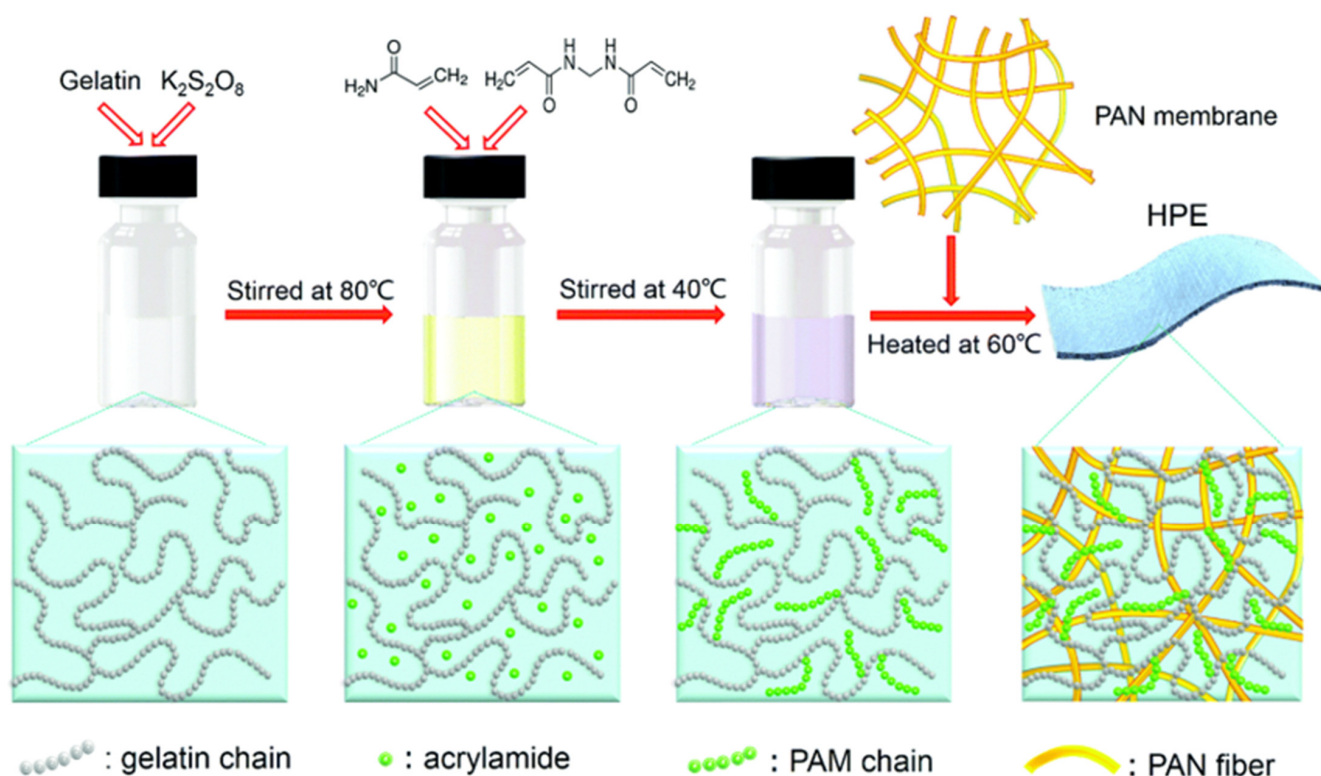


Figure 6. The synthesis route of the HPE. Reproduced with permission from [53].

The polymeric architecture of SPE is essential to engineer as it constructs the pathway of ion transportation and also polymer mobility that provides mechanical stability. Qiu et al. [54] developed a zwitterionic triple-network structure hydrogel electrolyte incorporating PAM, gelatin, and [(2-methylacryloxy)ethyl]dimethyl-(3-sulfonic acid propyl)ammonium hydroxide (DMAPS) for a flexible ZIB. The SPE was fabricated using a facile approach, as revealed in Figure 7a, where the mixture was polymerised at 60 °C and refrigerated. In terms of electromechanical efficiency, the addition of DMAPS on PAM/gelatin ZIBs caused an ionic conductivity of $3.51 \times 10^{-2} \text{ S cm}^{-1}$ to be achieved. This can be attributed to the addition of ion transportation pathways offered by the intrinsic zwitterionic groups on polymer chains, thus effectively accelerating the rate of ion transport. The PAM/gelatin/DMAPS electrolyte also revealed a self-healing ability owing to the hydrogen bond interaction and delivered an excellent coulombic efficiency of over 99%. Additionally, the mechanical tests in Figure 7c,d suggested that the inclusion of gelatin improves the elasticity and the toughness of the electrolyte, while DMAPS reduces the elasticity and toughness owing to its poly-zwitterion characteristic.

Dueramae et al. [55] proposed an innovative polymer electrolyte from carboxymethyl cellulose (CMC) and poly(N-isopropylacrylamide) (PNiPAM) as an SPE for ZIBs, which was synthesised via the solution casting method. As a result, the blended CMC/PNiPAM SPEs revealed magnificent performance in tensile strength (37.9 MPa) and modulus (2.1 GPa). The observed increase in film stiffness upon the addition of PNiPAM can be ascribed to the enhanced rigidity resulting from the presence of both -NH and -OH groups within PNiPAM. These functional groups actively engage in robust intermolecular bonding and electrostatic interactions with the carboxyl and hydroxyl groups of CMC. The nature of these interactions encompasses hydrogen bonding, dipole-dipole interactions, as well as charge effects. Collectively, these interactions contribute to the overall reinforcement of the film structure, leading to increased stiffness. Moreover, the thermal stability of the

CMC/PNiPAM was also examined, and the blended SPE was thermally more stable with a higher decomposition temperature compared to the pure CMC. The enhancement in thermal stability was suggested to be offered by the restricted chain motion between the respective functional groups of the CMC and PNiPAM molecules. The SPEs exhibited a moderate ionic conductivity of $1.68 \times 10^{-4} \text{ S cm}^{-1}$ and a high Zn^{2+} ion transference number of 0.56. This can be due to the porous structure of the SPE, which promotes zinc movement in the SPEs containing zinc triflate.

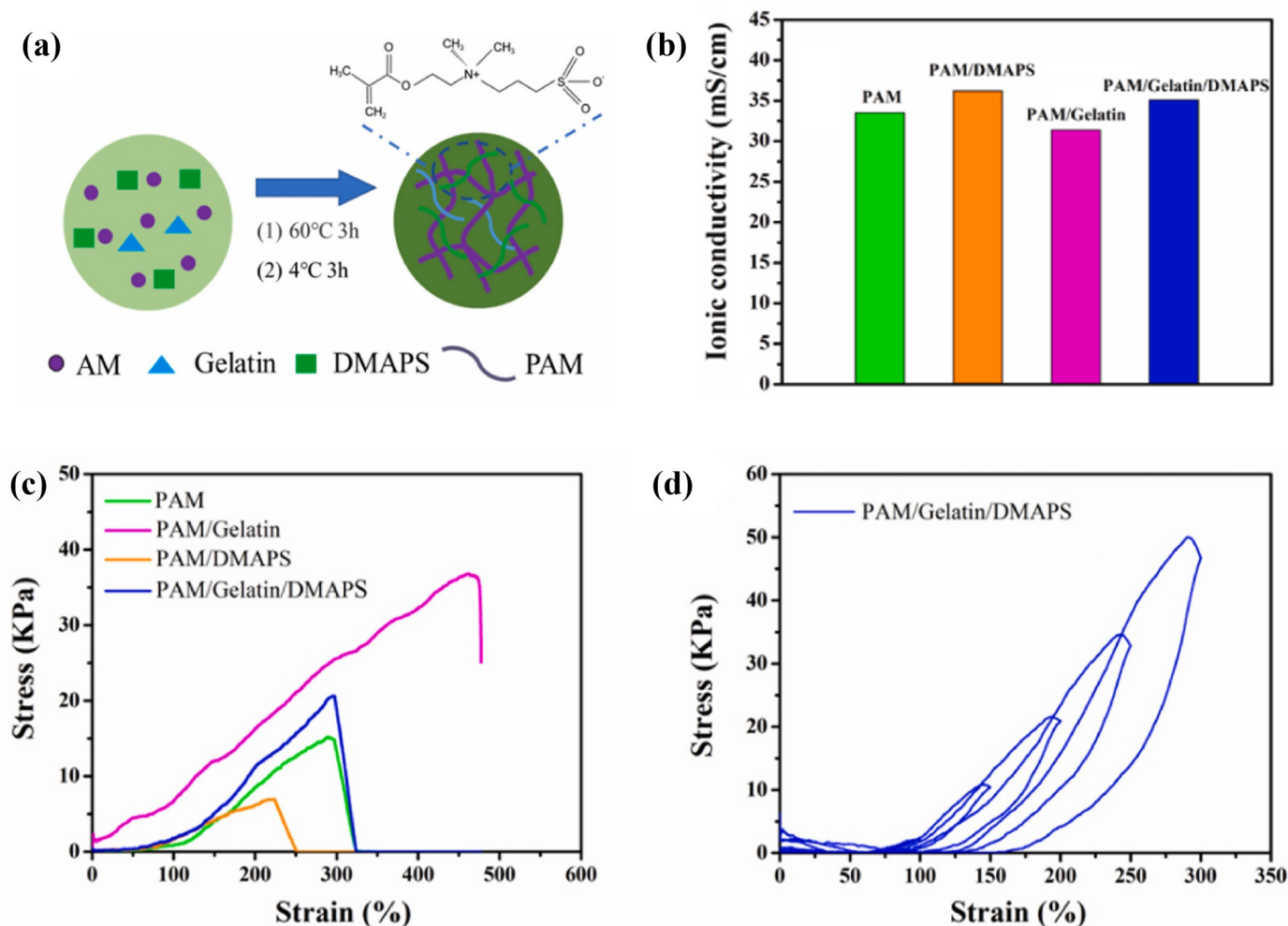


Figure 7. (a) Demonstrations of the synthesis process of the hydrogel. (b) The ionic conductivity of hydrogels with different compositions. (c) The tensile-stress-strain curves of the hydrogels. (d) The cycling loading-unloading curves of the hydrogel. Reproduced with permission from [54].

Among the reviews, bio-based polymers such as gelatin, cellulose, and gums have generally exhibited favourable electromechanical properties due to their intrinsic polymer structure. For instance, the linear chains with carboxymethyl substitution of CMC not only provide high mechanical flexibility and stability, but also create aligned charge transport paths. To further increase the biocompatibility of SPEs, Zhou et al. [56] developed a cellulose aerogel-gelatin (CAG) solid electrolyte for an implantable, biodegradable transient zinc-ion battery (TZIB). As shown in Figure 8, the gelatin electrolyte was grafted into a cellulose aerogel (CA) 3D porous framework via a super-assembly strategy. Subsequently, the 3D CA architecture was obtained via freeze-drying and pristine gelatin chain injection. The TZIB was then fabricated from a flexible silk protein film, in situ-evaporated Au film, screen-printed Zn film, and MnO_2/rGO hybrid materials as the encapsulation layer, collector, cathode, and anode materials, respectively.

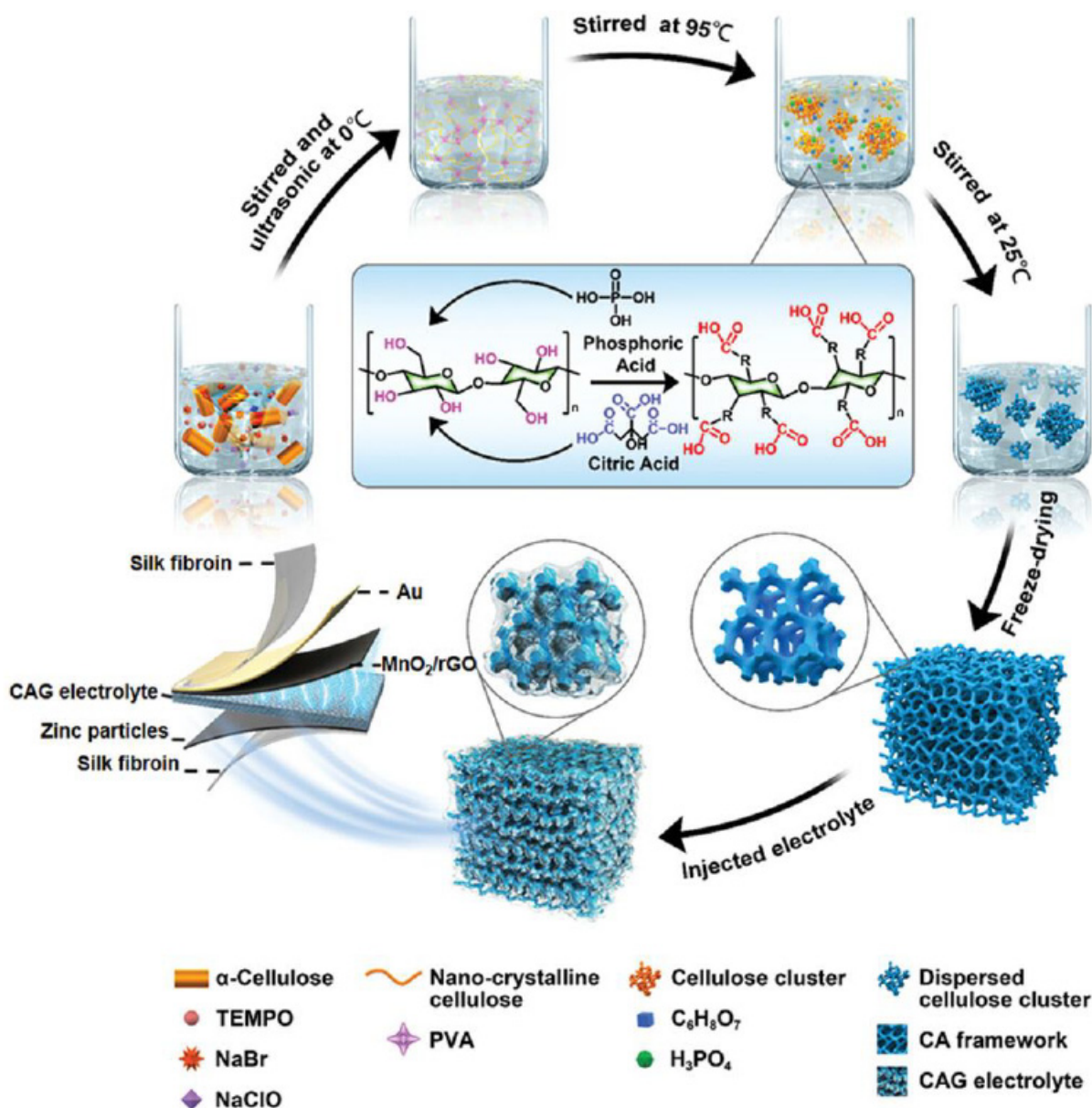


Figure 8. Demonstration of the super-assembly synthesis process. Reproduced with permission from [56].

As a result, the synthesised CAG film exhibited a highly porous three-dimensional (3D) structure, as illustrated in Figure 9a, possessing a significant liquid storage capacity. This unique structure endowed an extremely high ionic conductivity of $1.23 \times 10^{-2} \text{ S cm}^{-1}$ at ambient temperature while retaining great mechanical robustness (i.e., bending angle $> 120^\circ$) and biodegradability. The porous 3D framework plays a crucial role in enhancing electrolyte absorption and reinforcing the TZIB body. Furthermore, the presence of micropores facilitates the migration of electrolyte ions. The TZIB based on the CAG film exhibited favourable cyclability performance, ensuring both implantability and biodegradability. Even after 15 cycles, the capacity retention remained at 96.4%, and it maintained 95.4% capacity after being subjected to bending or folding. Moreover, the TZIB can be effectively biodegraded by phosphate-buffered saline (PBS) solution within a 30-day period, as demonstrated in Figure 9f. Importantly, the degradation materials of TZIB do not contain any heavy metal ions, toxic polymers, or electrolytes that could adversely affect human health. This characteristic positions TZIB as a potential candidate for self-powered transient electronics or conventional self-powered implantable medical devices in future applications.

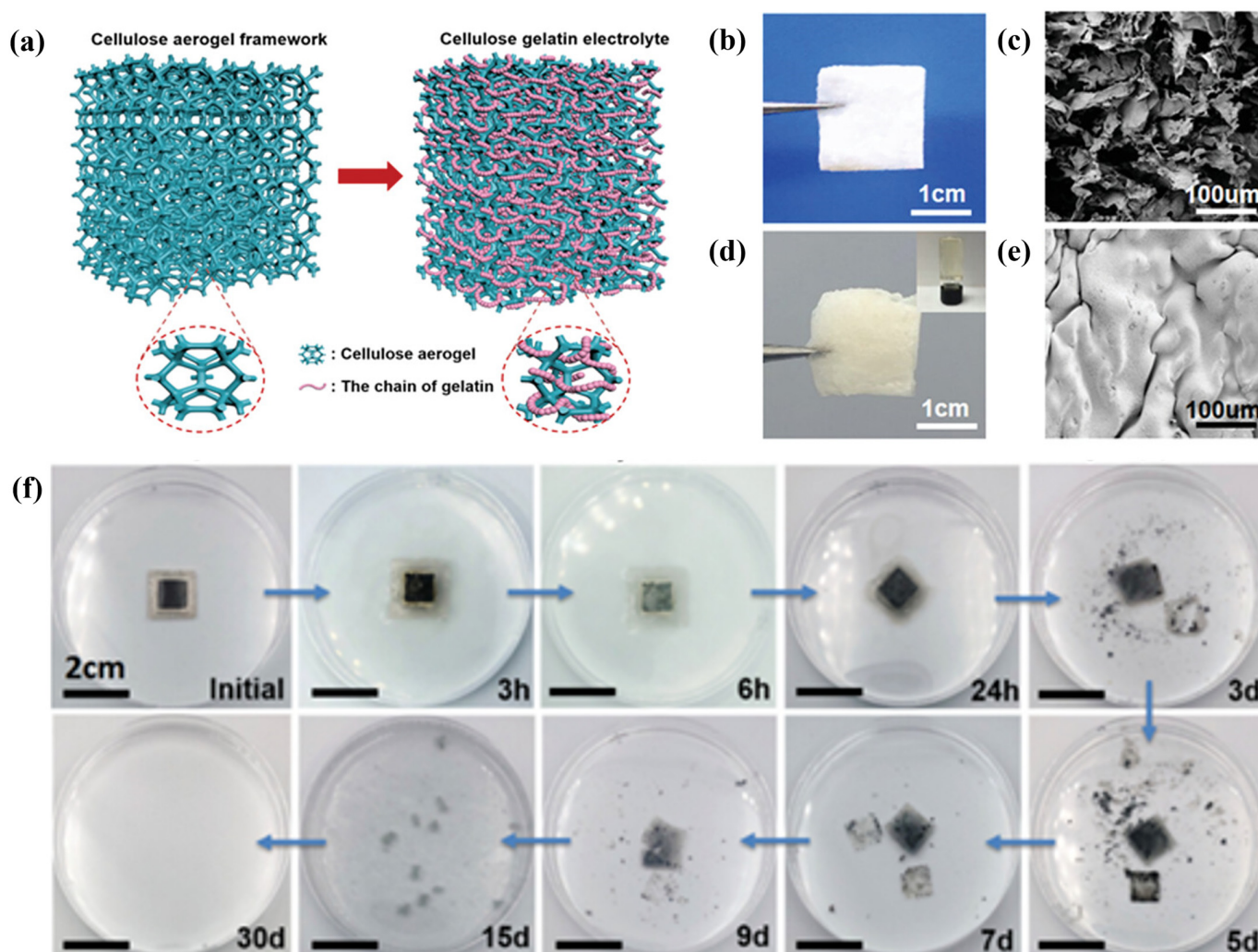


Figure 9. (a) Schematic diagrams of the structure and assembly of the CAG SPE. (b,c) The optical and SEM images of the CA framework. (d,e) Both optical and SEM photos of the fabricated CAG film. (f) Series of photos recording the biodegradation profile of the encapsulated battery in buffered protease solution at 37 °C. Reproduced with permission from [56].

Similar research also conducted by Zhou et al. [57] shows the fabrication of TZIB devices, including a plasticised gelatin-silk fibroin electrolyte film and a dual-yarn electrode structure. The gelatin-based electrolyte was synthesised as illustrated in Figure 10, where the gelatin solution was mixed with dissolved silk fibre. After ultrasonic treatment, the gelatin electrolyte was placed on the gelatin-silk film to obtain solidified film via rapid cooling to room temperature. Throughout the synthesis process, the polypeptide backbone of the silk protein underwent molecular conformational changes, dispersing among the doped gelatin chains in formic acid. Subsequently, as the acid volatilised, a plasticised silk protein film was formed. Over time, the gelatin molecule would gradually transit from a randomly coiled state to an ordered triple-helix structure. This structural arrangement facilitated the incorporation of β -sheets, endowed with robust mechanical properties, uniformly embedded within the gelatin-protein composite network, resulting in a homogeneous biomass composite framework. Consequently, the transient zinc-ion battery (TZIB) exhibited a high specific capacity of 311.7 mAh g^{-1} and excellent cycle stability with a capacity retention of 94.6% after 100 cycles. This performance is attributed to the notable ionic conductivity of $5.68 \times 10^{-3} \text{ S cm}^{-1}$ at room temperature. Regarding mechanical stability, the TZIB device demonstrated significant shape plasticity, retaining 82.5% of its capacity after undergoing

80 bends. Furthermore, it exhibited commendable biodegradability, fully degrading within 45 days under enzyme digestion.

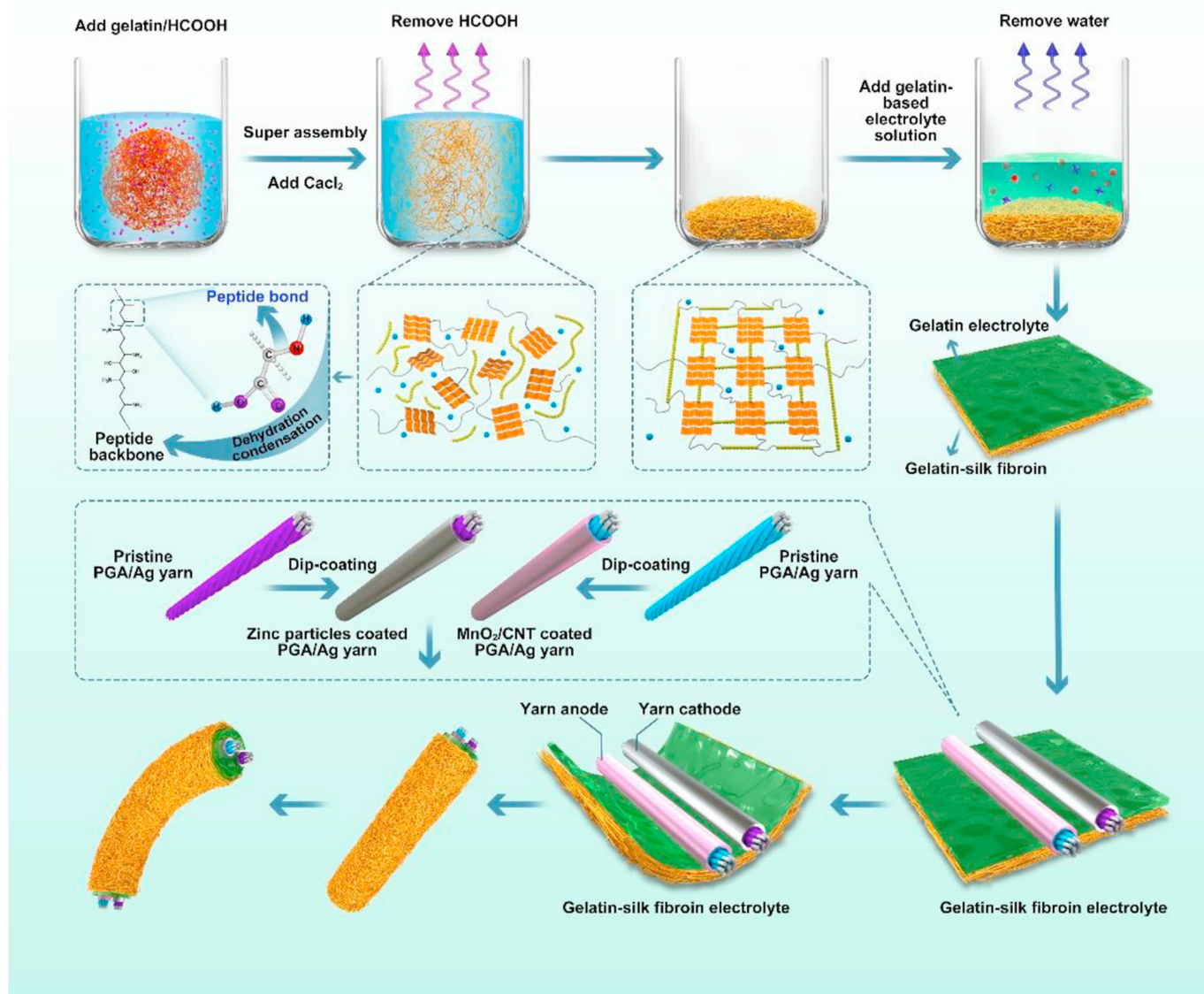


Figure 10. Schematic diagram of fabrication and encapsulation of the fibre-shaped TZIB. TZIB, transient zinc-ion battery. Reproduced with permission from [57].

Table 2 summarises the reviewed literature and studies in this section, including their molecular structures, ionic conductivity, features, and the published year. In general, the incorporation of the hybrid polymer system caused an enhancement in ionic conductivity, capacity retention, and mechanical flexibility, especially with the inclusion of a biopolymer (i.e., gelatin, cellulose). The intrinsic structure of these biopolymers can form unique 3D architectures with various polymer matrixes via crosslinking and polymerisation, such as heteroleptic [52], hierarchical [53], zwitterionic [54], and super-assembled porous structures [56]. These structures possess high porosity that increase the absorption of electrolytes, provide extra channels for the migration of electrolyte ions, and reinforce the integrity of the SPE by offering additional support in mechanical robustness. The engineered structures were even suggested to offer fast ligand exchanging and self-healing capacity owing to the hydrogen bond interaction. However, compared to the wide investigation in electromechanical efficiency, the improvement in mechanical modulus seems relatively impoverished; specifically, the uncontrollable growth of dendritic Zn during the cycling process has rarely

been discussed, as the dendrites may penetrate the polymer separator and raise safety risks that extremely restrict the further application [58,59].

Table 2. The molecular structure, ionic conductivity, and features of hybrid polymer matrix electrolyte.

Name	Molecule Structure	Ionic Conductivity (S cm ⁻¹)	Features	Year, Ref
PEO/PVDF		2.5×10^{-5}	<ul style="list-style-type: none"> Segmental mobility 	2017, [51]
PAAM/Acetamide		4.7×10^{-3}	<ul style="list-style-type: none"> Reversibility Cyclability 	2022, [52]
Gelatin/PAM		1.76×10^{-2}	<ul style="list-style-type: none"> High areal energy density Capacity retention of 97% after 1000 cycles Wearability 	2018, [53]
PAM/DMAPS/Gelatin		3.51×10^{-2}	<ul style="list-style-type: none"> Mechanical stability Flexible Excellent coulombic efficiency 	2022, [54]
CMC/PNiPAM		1.68×10^{-4}	<ul style="list-style-type: none"> Great tensile strength and modulus Flame retardant 	2020, [55]
Cellulose/Gelatin		1.23×10^{-2}	<ul style="list-style-type: none"> Biodegradable 	2022, [56]
Gelatin-silk fibroin		5.68×10^{-3}	<ul style="list-style-type: none"> Biodegradable Excellent cycle stability Shape plasticity 	2022, [57]
Lignin/Nafion		9.1×10^{-3}	<ul style="list-style-type: none"> Long cycle life 	2019, [60]
Cellulose/CMC		2.6×10^{-2}	<ul style="list-style-type: none"> Mechanical strength (70 MPa tensile strength) 95% capacity retention after 500 cycles 	2023, [61]

5. Nanocomposite Polymer Electrolytes

Except for incorporating various polymer matrices via cross-linking or polymerisation, including a small quantity of nanocomposites has also attracted research interests in enhancing the mechanical, thermal, electrical, and electrochemical properties of polymer electrolytes. This is owed to the distinctive microstructure with significant lateral dimensions and low thickness of the two-dimensional (2D) materials that endows a significant specific surface area and thermal/electrical conductivities. Sownthari and Austin Suthanthiraraj [62] employed organically modified montmorillonite (MMT) as an additive to enhance the electromechanical properties of a poly(ϵ -caprolactone) (PCL)-based electrolyte via the solution casting method. With 15 wt% of MMT, the modified MMT-PCL electrolyte acquired a moderate ionic conductivity of $9.5 \times 10^{-5} \text{ S cm}^{-1}$. This can be attributed to the enhanced dissociation of ion pairs and higher aggregates of dopant salt facilitated by the high dielectric constant of the nanoclay, where the number of free triflate ions increases the number of free Zn^{2+} for conduction. However, the MMT-PCL showed unsatisfied thermal stability, where an earlier decomposition temperature was observed due to the decrease in the electron density caused by the interaction of Zn^{2+} ions with the carbonyl oxygen. To investigate the feasibility of applying nanofillers into a hybrid polymer matrix, Prasanna and Suthanthiraraj [63] incorporated zirconia (ZrO_2) nanofillers into a poly(vinyl chloride)(PVC)/poly(ethyl methacrylate) (PEMA)-based GPE also via the solution casting method. As a result, the 3 wt% of ZrO_2 dispersed in PVC (30 wt%)/PEMA (70 wt%) GPE achieved an enhanced ionic conductivity at $3.63 \times 10^{-4} \text{ S cm}^{-1}$. The enhanced conductivity observed can be attributed to the Lewis-acid–base interaction between the electrolytic species and the OH/O sites present on the surface of the filler. This interaction creates additional hopping sites and conductive pathways for the migrating charged species, facilitating their movement within the system. Furthermore, the introduction of ZrO_2 into the electrolyte has the effect of enhancing the flexibility of the polymer chains. This is achieved by impeding the reorganisation of the chains and stabilising the amorphous phase of the composite gel polymer electrolyte (GPE). The increased flexibility and stabilisation contribute to improved performance and overall characteristics of the GPE.

To further strengthen the electromechanical performance of the nanofiller-infused electrolyte, Chen et al. [64] successfully developed a SPE for high-performance all-solid-state zinc-ion batteries (ZIBs) by employing a blade casting method. The SPE is based on the poly(vinylidene fluoride-co-hexafluoropropylene) matrix, which is filled with poly(methyl acrylate)-grafted MXenes. The composite material, denoted as PVHF/MXene-g-PMA, demonstrates remarkable stability and reliability in ZIB applications. MXene, as a relatively recent addition to the family of two-dimensional (2D) materials, shows tremendous potential as an advanced inorganic filler. It is represented by the chemical formula $\text{M}_{n+1}\text{X}_n\text{T}_x$, where M represents a transition metal, X represents carbon or nitrogen, and T represents a terminating group (O, OH, or F). MXene stands out due to its expansive specific surface area and abundant surface functional groups, making it an attractive candidate for enhancing the material properties when incorporated as a filler. The fabrication process is shown in Figure 11a. Firstly, LiF and HCL solution were employed to obtain 2D MXene by removing aluminium alloys. The PMA was then grafted with MXene via an in situ polymerisation on MXene surfaces, where the hydroxyl groups provide active grafting sites for the PMA. On the other hand, F-H hydrogen bonds can also be associated between PVHF and the H atoms of PMA. The resulting SPE with a PMA content of 0.05 exhibited an excellent ion conductivity of $2.69 \times 10^{-4} \text{ S cm}^{-1}$ at room temperature, which is an ionic conductivity three orders of magnitude larger than that of the PVHF matrix owing to the high electrical conductivity of MXene. Importantly, the SPE is able to maintain significant ionic conductivities at different temperatures ranging from $-25 \text{ }^\circ\text{C}$ to $85 \text{ }^\circ\text{C}$, as revealed in Figure 11b. Mechanical-wise, Figure 11c suggests that the PVHF/MXene-g-PMA offers a significant enhancement in the elongation (60.1%), where the stress was mostly maintained at 13.2 MPa compared with the neat PVHF. Moreover, a significant coulombic efficiency of 98.9% was maintained for over 350 cycles in the cyclic stability tests. Dendrite-free Zn

plating/stripping with high reversibility was achieved over 1000 and 200 h of cycling at 25 °C and 55 °C, where a remarkable capacity retention was maintained above 90% after 10,000 cycles at room temperature for more than 90 days.

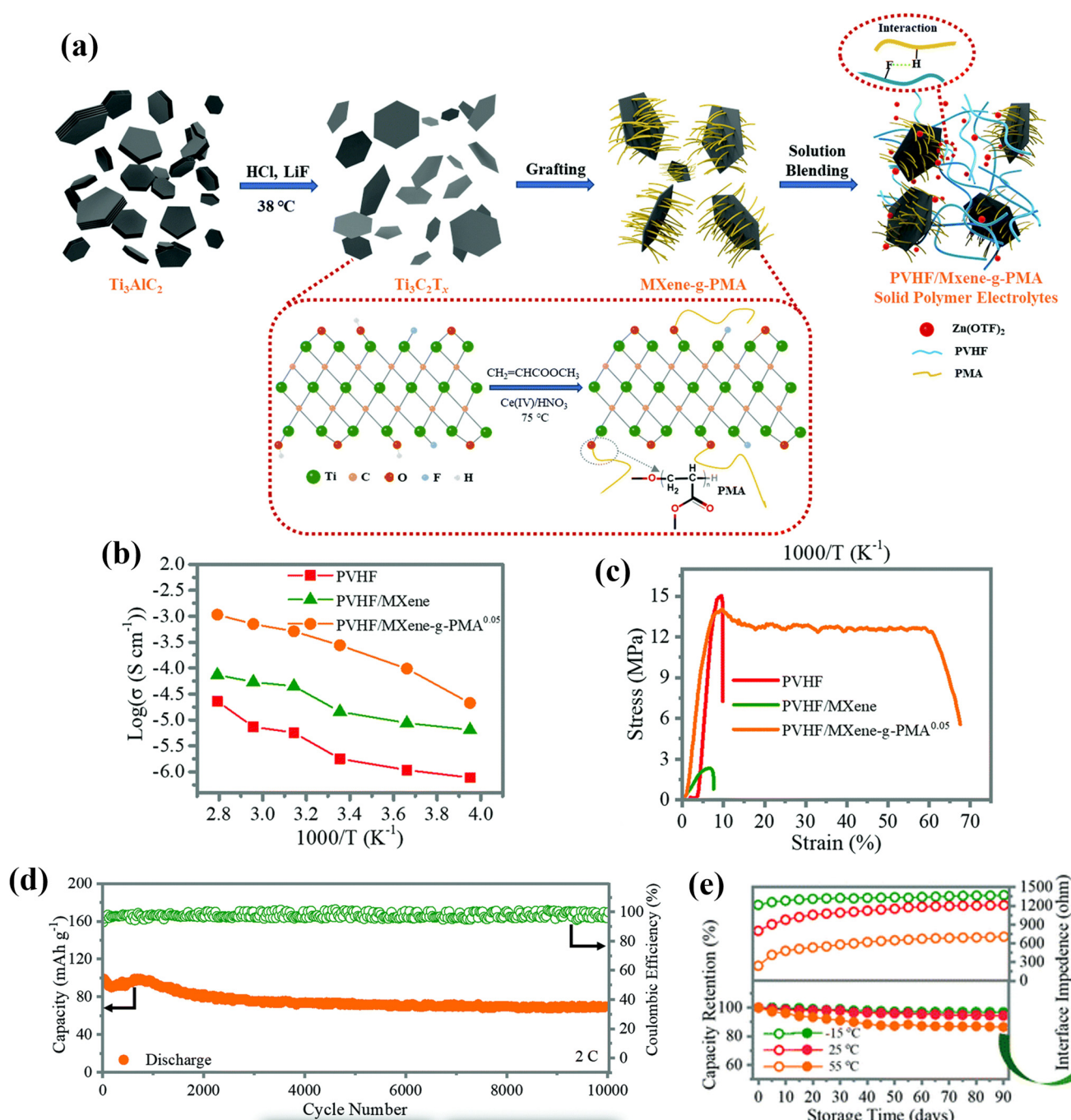


Figure 11. (a) The fabrication process of the PVHF/MXene-g-PMA SPEs. (b) Ionic conductivities at different temperatures. (c) Strain–stress curves. (d) Cycling performance and coulombic efficiency. (e) Capacity retention and interface impedance of the SPEs. Reproduced with permission from [64].

Liu et al. [65] reported a GPE for high-performance ZIBs employing MXene-derived TiO_2 nanosheets as an additive, which was obtained via hydrothermal reaction. The nanosheet was mixed with Polyvinyl alcohol (PVA) and $\text{Zn}(\text{CF}_3\text{SO}_3)_2$ in dissolved solution and frozen via the solution casting method, as revealed in Figure 12a. With 3 wt% of TiO_2 additives, the resulting GPE (PZ3T) exhibited a moderate ionic conductivity of $1.243 \times 10^{-5} \text{ S cm}^{-1}$ and excellent mechanical reinforcement, where the tensile strength

and elongation at break were significantly improved, as illustrated in Figure 12b. Importantly, the GPE also exhibited self-healing behaviour owing to the hydroxyl groups and hydrogen bonds between PVA chains and TiO_2 nanoparticles. Moreover, an excellent coulombic efficiency of 99.8% and stable and reversible Zn plating/stripping for over 3000 h were observed, attributed to the dendrite suppression effect.

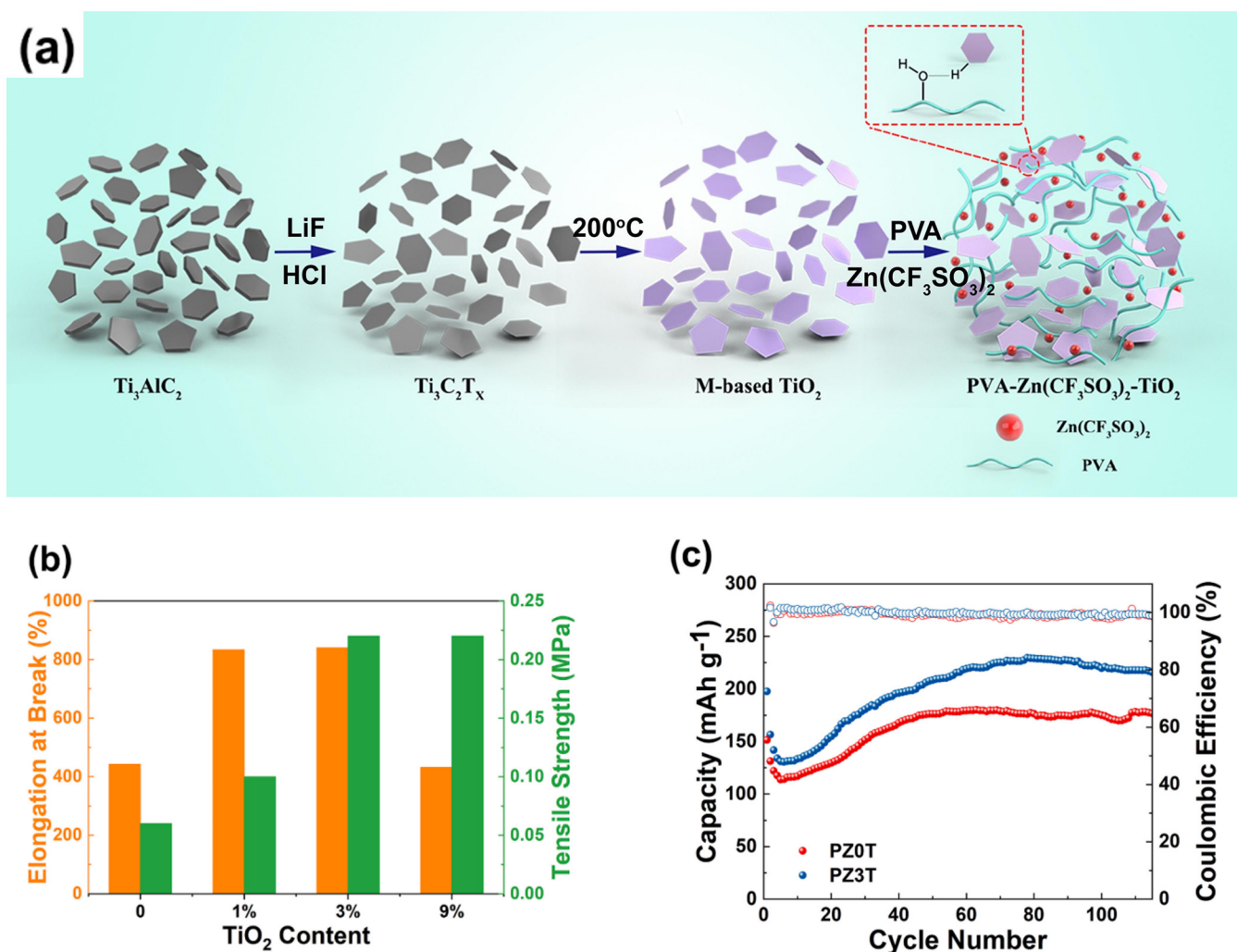
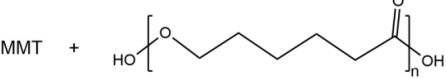
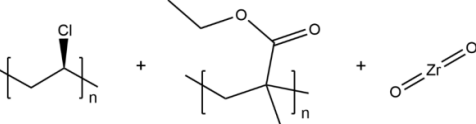


Figure 12. (a) The synthesis process of the TiO_2 -based GPE derived from MXene; (b) the percentage of elongation at break and tensile strength with contents of additives; (c) the cycling performance and coulombic efficiency of GPEs. Reproduced with permission from [65].

Table 3 summarises this section's reviewed literature and studies, including their molecular structures, ionic conductivity, features, and the published year. Compared to homogenous polymer and hybrid polymer matrix designs, the inclusion of nanoparticles into electrolytes for ZIBs is relatively rare and remains unexplored. In general, the addition of nanomaterials would offer an advancement to both the electromechanical and mechanical robustness of the SPEs, where the nano-fillers are able to pave additional ion migration pathways on the filler surface and reduce the crystallinity of the polymer [66]. MXene has exhibited astonishing electromechanical performance throughout the review, including capacity retention, long-life cycling, and self-healing mechanisms. Furthermore, it significantly reinforces the structural integrity of the polymer in elongation and tensile strength, enabling MXene as an anti-corrosion elastic constraint (AEC) against zinc dendrites by inducing uniform zinc deposition on the smooth surface of the TiO_2 -based SPE.

Table 3. The molecular structure, ionic conductivity, and features of nanocomposite electrolytes.

Name	Molecule Structure	Ionic Conductivity (S cm ⁻¹)	Feature	Year, Ref
MMT/PCL	MMT + 	9.5×10^{-5}	<ul style="list-style-type: none"> • Biodegradable • Weakened thermal stability 	2015, [62]
PVC/PEMA/ZrO ₂		3.63×10^{-4}	<ul style="list-style-type: none"> • Moderate thermal stability 	2019, [63]
PVHF/Mxene/PMA		2.69×10^{-4}	<ul style="list-style-type: none"> • Excellent capacity retention • Wide range of operational temperature • Long-life cycling 	2021, [64]
PVA/TiO ₂		1.243×10^{-5}	<ul style="list-style-type: none"> • Reinforcement in mechanical stability • Self-healing 	2022, [65]

6. Summary and Perspectives

In this review, we have discussed the state-of-the-art development of solid polymer electrolytes for zinc-ion batteries. We have highlighted the cutting-edge technologies of using SPEs in zinc-ion batteries, including their high safety, low cost, and potential for high-energy-density applications. Different routes employing polymer and polymer composites as SPEs to realise high-performance and safe zinc-ion batteries are also introduced and discussed, including homogenous polymer SPEs, hybrids polymer SPEs, and nanocomposites polymer SPEs.

In terms of the homogenous polymer SPEs, polymers like PEO, PVdF, PAM, and PVA can improve ionic conductivity and may be used to be part of the SPEs and applied in ZIBs. Unfortunately, the relatively low ionic conductivity seriously restricts further practical applications. Among them, SPEs containing bio-based polymers show good mechanical properties and promising electrical chemical properties when applied in ZIBs, which are attracting abroad attention.

On top of homogenous polymer SPEs, the addition of other functional polymers can obviously improve the ionic conductivity and tensile strength and can endow ZIBs with excellent electrochemical performance. The combination of various polymers can integrate different functions from each component and impart the SPEs' outstanding compatibility with electrolytes. Usually, various polymers may form crosslinking, self-assembly structures that can significantly enhance the mechanical strength of SPEs, improve the ionic conductivity of ZIBs, and realise promising electrochemical properties and safety. Specifically, the mixing of polymer interfaces can induce the formation of ion/polymer interactions that would facilitate the movement of zinc ions and achieve great ion conductivity. In addition, the unique amorphous structure can also reduce the cohesive force of polymer blend chains and offer favourable segmental mobility that can improve ion mobility within the polymer blend electrolyte system. Surprisingly, biopolymers such as gelatin, gums, and cellulose play critical roles in hybrid polymer SPEs and can provide mechanical support, biocompatibility, and environmental friendliness. These SPEs with biopolymers exhibit favourable electrochemical properties due to their intrinsic features, e.g., the linear

chains with carboxymethyl substitution of CMC may provide high mechanical flexibility and stability and create aligned charge transport paths.

Lastly, for the polymer nanocomposites SPEs, the incorporation of nanomaterials will usually significantly improve the ionic conductivity and mechanical performance. Nanomaterials may interact with polymers and form interfaces inside the polymer/inorganic composites system that can act as pathways for the zinc ions and facilitate ionic transportation efficiency. Additionally, considering the intrinsic property of inorganic materials, the addition of inorganic materials can usually obviously improve the surface modulus of SPEs, which may improve the operating stability and battery safety. Also, the improved modulus of SPEs induced by inorganic materials will also benefit the suppression of zinc dendrites.

In summary, SPEs hold great promise for the development of safe, low-cost, and high-performance zinc-ion batteries. Polymer engineering plays key roles in resolving current issues encountered in the synthesis and design of SPEs applied in ZIBs. While there are still some issues remaining, below are some challenges and perspectives raised for reference.

1. In terms of SPEs, one of the major challenges is the low ionic conductivity at room temperature, which limits the performance of zinc-ion batteries. Normally, a high ionic conductivity will improve the efficiency of ion transportation that can help achieve great electrochemical performance and alleviate the reduction of zinc metal on the surface of the anode. To address this challenge, several strategies can be employed, including the incorporation of high-conductivity salts, functional polymers, and the use of nanocomposites.
2. Another challenge is the mechanical stability of SPEs. Most polymers used as SPEs are soft and easily deformable, which can result in the formation of dendrites and short-circuits in the battery. To address this challenge, several strategies can be employed, including the incorporation of rigid segments into the polymer backbone, the use of crosslinked polymers, and the use of ceramic fillers. According to the methods used for lithium metal batteries, the addition of inorganic materials can improve the Young's modulus of SPEs and efficiently suppress the growth of metal dendrites. Therefore, in terms of ZIBs, the principle can also be utilised to address the safety issue induced by zinc dendrites. To date, the related studies are very limited, so this strategy might be a promising method to improve the electrochemical property and safety of ZIBs in a future study.
3. Furthermore, the long-term stability of SPEs needs to be further improved. Many SPEs undergo degradation over time due to the presence of the electrochemical active species, which can lead to the deterioration of ionic conductivity and capacity. Crosslinking and in situ polymerisation methods would be reasonable methods to improve the chemical and thermal stability of the SPEs. Additionally, the incorporation of inorganic nanomaterials would also help enhance the stability of SPEs attributed to the stability of the crystalline structures.
4. Lastly, biomass-based SPEs show promising potential in improving the ionic conductivity, biocompatibility, and stability of the ZIBs. Biomass polymers or macromolecules usually contain plenty of functional groups, which can provide lots of active sites that can interact with zinc salts and electrolytes. Therefore, biomass-based SPEs can show great compatibility with zinc salts and electrolytes and thus have very stable crosslinking structures and ion channels. These advantages enable biomass-based SPEs as a research hotspot for high-performance and safe ZIBs.

Author Contributions: Conceptualization, I.M.D.C.C. and W.W.; methodology, W.W.; software, W.W.; formal analysis, A.L. and B.L.; investigation, I.M.D.C.C.; resources, W.W., D.X.M. and L.X.; writing—original draft preparation, I.M.D.C.C. and W.W.; writing—review and editing, I.M.D.C.C. and W.W.; visualization, B.L.; supervision, W.W. and A.L.-S.E.; project administration, A.L.-S.E. All authors have read and agreed to the published version of the manuscript.

Funding: This research was supported under the Australian Research Council/Discovery Early Career Researcher Award (DECRA) funding scheme (project number DE230100180).

Data Availability Statement: Not applicable.

Conflicts of Interest: The authors declare no conflict of interest. The authors declare that they do not have any competing financial interests or personal relationships that might influence their work.

References

1. Ma, L.; Schroeder, M.A.; Pollard, T.P.; Borodin, O.; Ding, M.S.; Sun, R.; Cao, L.; Ho, J.; Baker, D.R.; Wang, C. Critical factors dictating reversibility of the zinc metal anode. *Energy Environ. Mater.* **2020**, *3*, 516–521. [[CrossRef](#)]
2. Brige, A.; Olsson, M.; Xiong, S.; Matic, A. A comparative study of hydroxyethylcellulose-based solid polymer electrolytes for solid state Zn batteries. *Nano Sel.* **2022**, *4*, 102–111. [[CrossRef](#)]
3. Chuai, M.; Yang, J.; Tan, R.; Liu, Z.; Yuan, Y.; Xu, Y.; Sun, J.; Wang, M.; Zheng, X.; Chen, N. Theory-Driven Design of a Cationic Accelerator for High-Performance Electrolytic MnO₂-Zn Batteries. *Adv. Mater.* **2022**, *34*, 2203249. [[CrossRef](#)] [[PubMed](#)]
4. Wang, G.; Kohn, B.; Scheler, U.; Wang, F.; Oswald, S.; Löffler, M.; Tan, D.; Zhang, P.; Zhang, J.; Feng, X. A High-Voltage, Dendrite-Free, and Durable Zn-Graphite Battery. *Adv. Mater.* **2020**, *32*, 1905681. [[CrossRef](#)]
5. Zuo, Y.; Wang, K.; Pei, P.; Wei, M.; Liu, X.; Xiao, Y.; Zhang, P. Zinc dendrite growth and inhibition strategies. *Mater. Today Energy* **2021**, *20*, 100692. [[CrossRef](#)]
6. Yang, Q.; Li, Q.; Liu, Z.; Wang, D.; Guo, Y.; Li, X.; Tang, Y.; Li, H.; Dong, B.; Zhi, C. Dendrites in Zn-based batteries. *Adv. Mater.* **2020**, *32*, 2001854. [[CrossRef](#)]
7. Lu, W.; Xie, C.; Zhang, H.; Li, X. Inhibition of zinc dendrite growth in zinc-based batteries. *ChemSusChem* **2018**, *11*, 3996–4006. [[CrossRef](#)]
8. Cao, Z.; Zhu, X.; Xu, D.; Dong, P.; Chee, M.O.L.; Li, X.; Zhu, K.; Ye, M.; Shen, J. Eliminating Zn dendrites by commercial cyanoacrylate adhesive for zinc ion battery. *Energy Storage Mater.* **2021**, *36*, 132–138. [[CrossRef](#)]
9. Yang, Z.; Lv, C.; Li, W.; Wu, T.; Zhang, Q.; Tang, Y.; Shao, M.; Wang, H. Revealing the Two-Dimensional Surface Diffusion Mechanism for Zinc Dendrite Formation on Zinc Anode. *Small* **2022**, *18*, 2104148. [[CrossRef](#)]
10. Ruan, P.; Liang, S.; Lu, B.; Fan, H.J.; Zhou, J. Design strategies for high-energy-density aqueous zinc batteries. *Angew. Chem.* **2022**, *134*, e202200598. [[CrossRef](#)]
11. Dang, J.; Yin, M.; Pan, D.; Tian, Z.; Chen, G.; Zou, J.; Miao, H.; Wang, Q.; Yuan, J. Four-functional iron/copper sulfide heterostructure for alkaline hybrid zinc batteries and water splitting. *Chem. Eng. J.* **2023**, *457*, 141357. [[CrossRef](#)]
12. Li, Y.; Wang, Z.; Cai, Y.; Pam, M.E.; Yang, Y.; Zhang, D.; Wang, Y.; Huang, S. Designing Advanced Aqueous Zinc-Ion Batteries: Principles, Strategies, and Perspectives. *Energy Environ. Mater.* **2022**, *5*, 823–851. [[CrossRef](#)]
13. Song, M.; Tan, H.; Chao, D.; Fan, H.J. Recent advances in Zn-ion batteries. *Adv. Funct. Mater.* **2018**, *28*, 1802564. [[CrossRef](#)]
14. Huang, J.; Wang, Z.; Hou, M.; Dong, X.; Liu, Y.; Wang, Y.; Xia, Y. Polyaniline-intercalated manganese dioxide nanolayers as a high-performance cathode material for an aqueous zinc-ion battery. *Nat. Commun.* **2018**, *9*, 2906. [[CrossRef](#)]
15. Wang, L.-P.; Wang, P.-F.; Wang, T.-S.; Yin, Y.-X.; Guo, Y.-G.; Wang, C.-R. Prussian blue nanocubes as cathode materials for aqueous Na-Zn hybrid batteries. *J. Power Sources* **2017**, *355*, 18–22. [[CrossRef](#)]
16. Fang, G.; Zhou, J.; Pan, A.; Liang, S. Recent advances in aqueous zinc-ion batteries. *ACS Energy Lett.* **2018**, *3*, 2480–2501. [[CrossRef](#)]
17. Ding, J.; Du, Z.; Gu, L.; Li, B.; Wang, L.; Wang, S.; Gong, Y.; Yang, S. Ultrafast Zn²⁺ intercalation and deintercalation in vanadium dioxide. *Adv. Mater.* **2018**, *30*, 1800762. [[CrossRef](#)]
18. Cai, Y.; Liu, F.; Luo, Z.; Fang, G.; Zhou, J.; Pan, A.; Liang, S. Pilotaxitic Na₁ 1V3O₇·9 nanoribbons/graphene as high-performance sodium ion battery and aqueous zinc ion battery cathode. *Energy Storage Mater.* **2018**, *13*, 168–174. [[CrossRef](#)]
19. Wan, F.; Niu, Z. Design strategies for vanadium-based aqueous zinc-ion batteries. *Angew. Chem.* **2019**, *131*, 16508–16517. [[CrossRef](#)]
20. Bósquez-Cáceres, M.F.; Hidalgo-Bonilla, S.; Morera Córdova, V.; Michell, R.M.; Tafur, J.P. Nanocomposite Polymer Electrolytes for Zinc and Magnesium Batteries: From Synthetic to Biopolymers. *Polymers* **2021**, *13*, 4284. [[CrossRef](#)]
21. Wu, K.; Huang, J.; Yi, J.; Liu, X.; Liu, Y.; Wang, Y.; Zhang, J.; Xia, Y. Recent advances in polymer electrolytes for zinc ion batteries: Mechanisms, properties, and perspectives. *Adv. Energy Mater.* **2020**, *10*, 1903977. [[CrossRef](#)]
22. Mo, F.; Guo, B.; Ling, W.; Wei, J.; Chen, L.; Yu, S.; Liang, G. Recent Progress and Challenges of Flexible Zn-Based Batteries with Polymer Electrolyte. *Batteries* **2022**, *8*, 59. [[CrossRef](#)]
23. Liu, D.; Tang, Z.; Luo, L.; Yang, W.; Liu, Y.; Shen, Z.; Fan, X.-H. Self-healing solid polymer electrolyte with high ion conductivity and super stretchability for all-solid zinc-ion batteries. *ACS Appl. Mater. Interfaces* **2021**, *13*, 36320–36329. [[CrossRef](#)] [[PubMed](#)]
24. Ma, T.; MacKenzie, J.D. Fully printed, high energy density flexible zinc-air batteries based on solid polymer electrolytes and a hierarchical catalyst current collector. *Flex. Pr. Electron.* **2019**, *4*, 015010. [[CrossRef](#)]
25. Lu, J.; Jaumaux, P.; Wang, T.; Wang, C.; Wang, G. Recent progress in quasi-solid and solid polymer electrolytes for multivalent metal-ion batteries. *J. Mater. Chem. A* **2021**, *9*, 24175–24194. [[CrossRef](#)]
26. Ma, L.; Chen, S.; Li, X.; Chen, A.; Dong, B.; Zhi, C. Liquid-Free All-Solid-State Zinc Batteries and Encapsulation-Free Flexible Batteries Enabled by In Situ Constructed Polymer Electrolyte. *Angew. Chem.* **2020**, *132*, 24044–24052. [[CrossRef](#)]

27. Zhu, J.; Yao, M.; Huang, S.; Tian, J.; Niu, Z. Thermal-Gated Polymer Electrolytes for Smart Zinc-Ion Batteries. *Angew. Chem. Int. Ed.* **2020**, *59*, 16480–16484. [[CrossRef](#)]
28. Fu, J.; Lee, D.U.; Hassan, F.M.; Yang, L.; Bai, Z.; Park, M.G.; Chen, Z. Flexible high-energy polymer-electrolyte-based rechargeable zinc–air batteries. *Adv. Mater.* **2015**, *27*, 5617–5622. [[CrossRef](#)]
29. Vijayakumar, V.; Ghosh, M.; Kurian, M.; Torris, A.; Dilwale, S.; Badiger, M.V.; Winter, M.; Nair, J.R.; Kurungot, S. An In Situ Cross-Linked Nonaqueous Polymer Electrolyte for Zinc-Metal Polymer Batteries and Hybrid Supercapacitors. *Small* **2020**, *16*, 2002528. [[CrossRef](#)]
30. Lin, C.; Shinde, S.S.; Li, X.; Kim, D.H.; Li, N.; Sun, Y.; Song, X.; Zhang, H.; Lee, C.H.; Lee, S.U. Solid-State Rechargeable Zinc–Air Battery with Long Shelf Life Based on Nanoengineered Polymer Electrolyte. *ChemSusChem* **2018**, *11*, 3215–3224. [[CrossRef](#)]
31. Liu, J.; Khanam, Z.; Muchakayala, R.; Song, S. Fabrication and characterization of Zn-ion-conducting solid polymer electrolyte films based on PVdF-HFP/Zn (Tf) 2 complex system. *J. Mater. Sci. Mater. Electron.* **2020**, *31*, 6160–6173. [[CrossRef](#)]
32. Wu, J.; Wang, Y.; Deng, D.; Bai, Y.; Liu, M.; Zhao, X.; Xiong, X.; Lei, Y. Low-temperature resistant gel polymer electrolytes for zinc–air batteries. *J. Mater. Chem. A* **2022**, *10*, 19304–19319. [[CrossRef](#)]
33. Zhang, Y.; Wu, D.; Huang, F.; Cai, Y.; Li, Y.; Ke, H.; Lv, P.; Wei, Q. “Water-in-Salt” Nonalkaline Gel Polymer Electrolytes Enable Flexible Zinc-Air Batteries with Ultra-Long Operating Time. *Adv. Funct. Mater.* **2022**, *32*, 2203204. [[CrossRef](#)]
34. Fan, X.; Liu, J.; Song, Z.; Han, X.; Deng, Y.; Zhong, C.; Hu, W. Porous nanocomposite gel polymer electrolyte with high ionic conductivity and superior electrolyte retention capability for long-cycle-life flexible zinc–air batteries. *Nano Energy* **2019**, *56*, 454–462. [[CrossRef](#)]
35. Fan, X.; Wang, H.; Liu, X.; Liu, J.; Zhao, N.; Zhong, C.; Hu, W.; Lu, J. Functionalized Nanocomposite Gel Polymer Electrolyte with Strong Alkaline-Tolerance and High Zinc Anode Stability for Ultralong-Life Flexible Zinc–Air Batteries. *Adv. Mater.* **2023**, *35*, 2209290. [[CrossRef](#)]
36. Hong, Z.; Ahmad, Z.; Viswanathan, V. Design principles for dendrite suppression with porous polymer/aqueous solution hybrid electrolyte for Zn metal anodes. *ACS Energy Lett.* **2020**, *5*, 2466–2474. [[CrossRef](#)]
37. Wang, Y.; Wang, Z.; Yang, F.; Liu, S.; Zhang, S.; Mao, J.; Guo, Z. Electrolyte Engineering Enables High Performance Zinc-Ion Batteries. *Small* **2022**, *18*, 2107033. [[CrossRef](#)] [[PubMed](#)]
38. Hansen, E.J.; Liu, J. Materials and structure design for solid-state zinc-ion batteries: A mini-review. *Front. Energy Res.* **2021**, *8*, 616665. [[CrossRef](#)]
39. Zhang, N.; Chen, X.; Yu, M.; Niu, Z.; Cheng, F.; Chen, J. Materials chemistry for rechargeable zinc-ion batteries. *Chem. Soc. Rev.* **2020**, *49*, 4203–4219. [[CrossRef](#)] [[PubMed](#)]
40. Hiralal, P.; Imaizumi, S.; Unalan, H.E.; Matsumoto, H.; Minagawa, M.; Rouvala, M.; Tanioka, A.; Amaratunga, G.A.J. Nanomaterial-enhanced all-solid flexible zinc–carbon batteries. *ACS Nano* **2010**, *4*, 2730–2734. [[CrossRef](#)]
41. Tafur, J.P.; Abad, J.; Román, E.; Romero, A.J.F.J.E.C. Charge storage mechanism of MnO₂ cathodes in Zn/MnO₂ batteries using ionic liquid-based gel polymer electrolytes. *ACS Nano* **2015**, *60*, 190–194.
42. Li, H.; Liu, Z.; Liang, G.; Huang, Y.; Huang, Y.; Zhu, M.; Pei, Z.; Xue, Q.; Tang, Z.; Wang, Y.J.A.n. Waterproof and tailorable elastic rechargeable yarn zinc ion batteries by a cross-linked polyacrylamide electrolyte. *ACS Nano* **2018**, *12*, 3140–3148. [[CrossRef](#)] [[PubMed](#)]
43. Kaltenbrunner, M.; Kettlgruber, G.; Siket, C.; Schwödiauer, R.; Bauer, S.J. Arrays of ultracompliant electrochemical dry gel cells for stretchable electronics. *Adv. Mater.* **2010**, *22*, 2065–2067. [[CrossRef](#)]
44. Yi, J.; Guo, S.; He, P.; Zhou, H.J.E. Status and prospects of polymer electrolytes for solid-state Li–O₂ (air) batteries. *Energy Environ. Sci.* **2017**, *10*, 860–884. [[CrossRef](#)]
45. Zhao, Z.; Wang, J.; Lv, Z.; Wang, Q.; Zhang, Y.; Lu, G.; Zhao, J.; Cui, G. In-situ formed all-amorphous poly (ethylene oxide)-based electrolytes enabling solid-state Zn electrochemistry. *Chem. Eng. J.* **2021**, *417*, 128096. [[CrossRef](#)]
46. Kumar, G. Electrochemical characterization of poly(vinylidene fluoride)-zinc triflate gel polymer electrolyte and its application in solid-state zinc batteries. *Solid State Ion.* **2003**, *160*, 289–300. [[CrossRef](#)]
47. Huang, Y.; Liu, J.; Zhang, J.; Jin, S.; Jiang, Y.; Zhang, S.; Li, Z.; Zhi, C.; Du, G.; Zhou, H. Flexible quasi-solid-state zinc ion batteries enabled by highly conductive carrageenan bio-polymer electrolyte. *RSC Adv.* **2019**, *9*, 16313–16319. [[CrossRef](#)] [[PubMed](#)]
48. Huang, Y.; Zhang, J.; Liu, J.; Li, Z.; Jin, S.; Li, Z.; Zhang, S.; Zhou, H. Flexible and stable quasi-solid-state zinc ion battery with conductive guar gum electrolyte. *Mater. Today Energy* **2019**, *14*, 100349. [[CrossRef](#)]
49. Wu, M.; Zhang, Y.; Xu, L.; Yang, C.; Hong, M.; Cui, M.; Clifford, B.C.; He, S.; Jing, S.; Yao, Y. A sustainable chitosan-zinc electrolyte for high-rate zinc-metal batteries. *Matter* **2022**, *5*, 3402–3416. [[CrossRef](#)]
50. Ye, H.; Xu, J.J. Zinc ion conducting polymer electrolytes based on oligomeric polyether/PVDF-HFP blends. *J. Power Sources* **2007**, *165*, 500–508. [[CrossRef](#)]
51. Rathika, R.; Padmaraj, O.; Suthanthiraraj, S.A. Electrical conductivity and dielectric relaxation behaviour of PEO/PVdF-based solid polymer blend electrolytes for zinc battery applications. *Ionics* **2017**, *24*, 243–255. [[CrossRef](#)]
52. Lu, G.; Qiu, H.; Du, X.; Sonigara, K.K.; Wang, J.; Zhang, Y.; Chen, Z.; Chen, L.; Ren, Y.; Zhao, Z.; et al. Heteroleptic Coordination Polymer Electrolytes Initiated by Lewis-Acidic Eutectics for Solid Zinc–Metal Batteries. *Chem. Mater.* **2022**, *34*, 8975–8986. [[CrossRef](#)]

53. Li, H.; Han, C.; Huang, Y.; Huang, Y.; Zhu, M.; Pei, Z.; Xue, Q.; Wang, Z.; Liu, Z.; Tang, Z.; et al. An extremely safe and wearable solid-state zinc ion battery based on a hierarchical structured polymer electrolyte. *Energy Environ. Sci.* **2018**, *11*, 941–951. [[CrossRef](#)]
54. Qiu, M.; Liu, H.; Tawiah, B.; Jia, H.; Fu, S. Zwitterionic triple-network hydrogel electrolyte for advanced flexible zinc ion batteries. *Compos. Commun.* **2021**, *28*, 100942. [[CrossRef](#)]
55. Dueramae, I.; Okhawilai, M.; Kasemsiri, P.; Uyama, H.; Kita, R. Properties enhancement of carboxymethyl cellulose with thermo-responsive polymer as solid polymer electrolyte for zinc ion battery. *Sci. Rep.* **2020**, *10*, 12587. [[CrossRef](#)] [[PubMed](#)]
56. Zhou, J.; Zhang, R.; Xu, R.; Li, Y.; Tian, W.; Gao, M.; Wang, M.; Li, D.; Liang, X.; Xie, L.; et al. Super-Assembled Hierarchical Cellulose Aerogel-Gelatin Solid Electrolyte for Implantable and Biodegradable Zinc Ion Battery. *Adv. Funct. Mater.* **2022**, *32*, 2111406. [[CrossRef](#)]
57. Zhou, J.; Li, Y.; Xie, L.; Xu, R.; Zhang, R.; Gao, M.; Tian, W.; Li, D.; Qiao, L.; Wang, T.; et al. Humidity-sensitive, shape-controllable, and transient zinc-ion batteries based on plasticizing gelatin-silk protein electrolytes. *Mater. Today Energy* **2021**, *21*, 100712. [[CrossRef](#)]
58. Wang, W.; Liao, C.; Liew, K.M.; Chen, Z.; Song, L.; Kan, Y.; Hu, Y.J.J.o.M.C.A. A 3D flexible and robust HAPs/PVA separator prepared by a freezing-drying method for safe lithium metal batteries. *J. Mater. Chem. A* **2019**, *7*, 6859–6868. [[CrossRef](#)]
59. Wang, W.; Yuen, A.C.Y.; Yuan, Y.; Liao, C.; Li, A.; Kabir, I.I.; Kan, Y.; Hu, Y.; Yeoh, G.H.J.C.E.J. Nano architected halloysite nanotubes enable advanced composite separator for safe lithium metal batteries. *Chem. Eng. J.* **2023**, *451*, 138496. [[CrossRef](#)]
60. Yuan, D.; Manalastas, W., Jr.; Zhang, L.; Chan, J.J.; Meng, S.; Chen, Y.; Srinivasan, M. Lignin@Nafion Membranes Forming Zn Solid-Electrolyte Interfaces Enhance the Cycle Life for Rechargeable Zinc-Ion Batteries. *ChemSusChem* **2019**, *12*, 4889–4900. [[CrossRef](#)]
61. Xu, L.; Meng, T.; Zheng, X.; Li, T.; Brozena, A.H.; Mao, Y.; Zhang, Q.; Clifford, B.C.; Rao, J.; Hu, L. Nanocellulose-Carboxymethylcellulose Electrolyte for Stable, High-Rate Zinc-Ion Batteries. *Adv. Funct. Mater.* **2023**, 2302098. [[CrossRef](#)]
62. Sownthari, K.; Suthanthiraraj, S.A. Preparation and properties of biodegradable polymer-layered silicate nanocomposite electrolytes for zinc based batteries. *Electrochim. Acta* **2015**, *174*, 885–892. [[CrossRef](#)]
63. Sai Prasanna, C.M.; Austin Suthanthiraraj, S. PVC/PEMA-based blended nanocomposite gel polymer electrolytes plasticized with room temperature ionic liquid and dispersed with nano-ZrO₂ for zinc ion batteries. *Polym. Compos.* **2019**, *40*, 3402–3411. [[CrossRef](#)]
64. Chen, Z.; Li, X.; Wang, D.; Yang, Q.; Ma, L.; Huang, Z.; Liang, G.; Chen, A.; Guo, Y.; Dong, B.; et al. Grafted MXene/polymer electrolyte for high performance solid zinc batteries with enhanced shelf life at low/high temperatures. *Energy Environ. Sci.* **2021**, *14*, 3492–3501. [[CrossRef](#)]
65. Liu, C.; Tian, Y.; An, Y.; Yang, Q.; Xiong, S.; Feng, J.; Qian, Y. Robust and flexible polymer/MXene-derived two dimensional TiO₂ hybrid gel electrolyte for dendrite-free solid-state zinc-ion batteries. *Chem. Eng. J.* **2022**, *430*, 132748. [[CrossRef](#)]
66. Lin, D.; Liu, W.; Liu, Y.; Lee, H.R.; Hsu, P.-C.; Liu, K.; Cui, Y. High ionic conductivity of composite solid polymer electrolyte via in situ synthesis of monodispersed SiO₂ nanospheres in poly (ethylene oxide). *Nano Lett.* **2016**, *16*, 459–465. [[CrossRef](#)]

Disclaimer/Publisher's Note: The statements, opinions and data contained in all publications are solely those of the individual author(s) and contributor(s) and not of MDPI and/or the editor(s). MDPI and/or the editor(s) disclaim responsibility for any injury to people or property resulting from any ideas, methods, instructions or products referred to in the content.